

EUR 3114.e

European Atomic Energy Community - EURATOM

FIAT S.p.A., Sezione Energia Nucleare - Torino

Società ANSALDO S.p.A. - Genova

AN INVESTIGATION ON SOME PARAMETERS INFLUENCING NON-UNIFORM HEAT FLUX DNB PREDICTION

by

G. PREVITI and M. DE BERNARDI
(FIAT)

1966



Contract No. 008-61-12 PNII

LEGAL NOTICE

This document was prepared under the sponsorship of the Commission of the European Atomic Energy Community (EURATOM).

Neither the EURATOM Commission, its contractors nor any person acting on their behalf :

Make any warranty or representation, express or implied, with respect to the accuracy, completeness, or usefulness of the information contained in this document, or that the use of any information, apparatus, method, or process disclosed in this document may not infringe privately owned rights; or

Assume any liability with respect to the use of, or for damages resulting from the use of any information, apparatus, method or process disclosed in this document.

This report is on sale at the addresses listed on cover page 4

at the price of FF 7,—	FB 70,—	DM 5,60	Lit. 870	FL 5,10
------------------------	---------	---------	----------	---------

When ordering, please quote the EUR number and the title, which are indicated on the cover of each report.

Printed by Guyot
Brussels, August 1966

This document was duplicated on the basis of the best available copy.

EUR 3114.e

AN INVESTIGATION ON SOME PARAMETERS INFLUENCING NON-UNIFORM HEAT FLUX DNB PREDICTION

by G. PREVITI and M. DE BERNARDI (FIAT)

European Atomic Energy Community - EURATOM
FIAT S.p.A., Sezione Energia Nucleare - Torino (Italy)
Società ANSALDO S.p.A. - Genova (Italy)
Contract No. 008-61-12 PNII
Brussels, August 1966 - 52 Pages - 19 Figures - FB 70

In nuclear reactor core thermal design only non-uniform axial heating must be considered. The shape of the heat flux distribution varies over the core lifetime; therefore it is important to be able to correctly predict the effect of non-uniform axial flux distribution on DNB (Departure from Nuclear Boiling).

Recent tests conducted by various laboratories have shown a marked influence of the heat flux distribution both on DNB power and location point.

EUR 3114.e

AN INVESTIGATION ON SOME PARAMETERS INFLUENCING NON-UNIFORM HEAT FLUX DNB PREDICTION

by G. PREVITI and M. DE BERNARDI (FIAT)

European Atomic Energy Community - EURATOM
FIAT S.p.A., Sezione Energia Nucleare - Torino (Italy)
Società ANSALDO S.p.A. - Genova (Italy)
Contract No. 008-61-12 PNII
Brussels, August 1966 - 52 Pages - 19 Figures - FB 70

In nuclear reactor core thermal design only non-uniform axial heating must be considered. The shape of the heat flux distribution varies over the core lifetime; therefore it is important to be able to correctly predict the effect of non-uniform axial flux distribution on DNB (Departure from Nuclear Boiling).

Recent tests conducted by various laboratories have shown a marked influence of the heat flux distribution both on DNB power and location point.

A correction factor, derived by a theoretical analysis, has been proposed in order to predict non uniform heat flux DNB conditions from corresponding uniform flux data.

Scope of the present work is to define the field of applicability of the theoretical approach to point out the role of some important parameter such DNB length and pressure and to modify the theoretical analysis for the high quality region.

An analytical expression for factor

$$C = \frac{h}{pV \cdot s \cdot C_p}$$

in bubbly flow region has been derived.

A correction factor, derived by a theoretical analysis, has been proposed in order to predict non uniform heat flux DNB conditions from corresponding uniform flux data.

Scope of the present work is to define the field of applicability of the theoretical approach to point out the role of some important parameter such DNB length and pressure and to modify the theoretical analysis for the high quality region.

An analytical expression for factor

$$C = \frac{h}{pV \cdot s \cdot C_p}$$

in bubbly flow region has been derived.

EUR 3114.e

European Atomic Energy Community - EURATOM

FIAT S.p.A., Sezione Energia Nucleare - Torino

Società ANSALDO S.p.A. - Genova

AN INVESTIGATION ON SOME PARAMETERS INFLUENCING NON-UNIFORM HEAT FLUX DNB PREDICTION

by

G. PREVITI and M. DE BERNARDI
(FIAT)

1966



SUMMARY

In nuclear reactor core thermal design only non-uniform axial heating must be considered. The shape of the heat flux distribution varies over the core lifetime; therefore it is important to be able to correctly predict the effect of non-uniform axial flux distribution on DNB (Departure from Nuclear Boiling).

Recent tests conducted by various laboratories have shown a marked influence of the heat flux distribution both on DNB power and location point.

A correction factor, derived by a theoretical analysis, has been proposed in order to predict non uniform heat flux DNB conditions from corresponding uniform flux data.

Scope of the present work is to define the field of applicability of the theoretical approach to point out the role of some important parameter such DNB length and pressure and to modify the theoretical analysis for the high quality region.

An analytical expression for factor

$$C = \frac{h}{pV s C_p}$$

in bubbly flow region has been derived.

TABLE OF CONTENTS

	Page No.
LIST OF FIGURES	I
LIST OF TABLES	II
NOMENCLATURE	III
 1. <u>INTRODUCTION</u>	 1
2. <u>THEORETICAL ANALYSIS</u>	2
2.a - BUBBLY FLOW	2
2.a.1 - Theoretical evaluation of factor C for bubbly flow regime	 5
a. Heat transfer coefficient "h"	5
b. Velocity of superheated liquid layer	8
c. Thickness of liquid layer "s"	8
2.a.2 - Influence of DNB length on non uniform heat flux prediction (bubble flow region)	 10
2.b - ANNULAR FLOW.	14
 REFERENCES.	 19

- - - - -

LIST OF FIGURES

- FIG. 1 - Physical Model of superheated liquid layer between bubble layer and Heating Surface (from references 6).
- FIG. 2 - Effect of power distribution on burnout-critical power versus quality at DNB location.
- FIG. 3 - Effect of power distribution on burnout-critical power versus quality at DNB location.
- FIG. 4 - Effect of power distribution on burnout-critical power versus quality at DNB location.
- FIG. 5 - Effect of power distribution on burnout-critical power versus quality at DNB location.
- FIG. 6 - Effect of power distribution on burnout-critical power versus quality at DNB location.
- FIG. 7 - Boiling curve of partial boiling.
- FIG. 8 - Heat flux distribution (reference 2).
- FIG. 9 - Comparison of measured and predicted values of correction factor (F) for heat flux data from reference (2), FIAT METHOD.
- FIG.10 - Comparison of measured and predicted values of correction factor (F) for heat flux data from reference (2), REF.(6) METHOD.
- FIG.11 - Comparison of measured and predicted values of correction factor (F) for heat flux data from reference (2), REF.(6) METHOD WITH MODIFIED L.
- FIG.12 - Comparison of measured and predicted values of correction factor (F) for cosine heat flux data from reference (3), FIAT METHOD.
- FIG.13 - Comparison of measured and predicted values for correction factor (F) for cosine heat flux data from reference (3), REF.(6) METHOD.
- FIG.14 - Physical Model of annular flow.
- FIG.15 - NON UNIFORM HEAT FLUX DISTRIBUTION, REFERENCE (5).
- FIG.16 - NON UNIFORM HEAT FLUX DISTRIBUTION, REFERENCE (3), (17).
- FIG.17 - Comparison of measured and predicted values of correction factor (F) for annular flow regime with FIAT "Ca".
- FIG.18 - Comparison of measured and predicted values of correction factor (F) for annular flow regime with "C" from reference (6).
- FIG.19 - Comparison of measured and predicted values of correction factor (F) for annular flow regime with "C" from reference (5).

LIST OF TABLES

TABLE 1	-	DATA
TABLE 2	-	RESULTS
TABLE 3	-	DATA - ANNULAR REGION
TABLE 4	-	RESULTS - ANNULAR REGION

* * * *

NOMENCLATURE

a	: exponent defined in text (-)
C, C _t , C _F , C _a	: coefficient defined in text (L ⁻¹)
C _p	: specific heat of superheated liquid ($\frac{E}{M \theta}$)
C _{pL}	: specific heat of liquid crossing the bubble layer ($\frac{E}{M \theta}$)
D	: diameter (L)
D _e	: equivalent diameter (L)
E	: rate of liquid re-entrainment ($\frac{M}{L^2 T}$)
F	: correction factor, defined in text (-)
G	: mass velocity ($\frac{M}{L^2 T}$)
G	: axial mass velocity ($\frac{M}{L^2 T}$)
h	: heat transfer coefficient from superheated layer to bubble layer ($\frac{E}{L^2 T \theta}$)
H	: enthalpy ($\frac{E}{M}$)
H _Z	: enthalpy at Z point (E/M)
H _{SAT}	: enthalpy of saturated liquid or of the bubble layer (E/M)
H _{fg}	: enthalpy of vaporization (E/M)
K	: actual pressure loss coefficient (-)
K	: pressure loss coefficient without axial inertia (-)
l	: length (L)
l _{DNB}	: distance from inception of local boiling or from point of bubble detachment to point of DNB (L)
l _{DNB.U}	: l _{DNB} for uniform flux (L)
l _{DNB.N.U}	: l _{DNB} for non uniform flux (L)
P	: perimeter of heater (L)

p	: pressure (F/L^2)
q''	: heat flux ($\frac{E}{L^2 T}$)
q''_t	: heat flux from superheated layer to bubble layer ($\frac{E}{L^2 T}$)
$q''_{DNB,loc}$: critical local heat flux at DNB point ($\frac{E}{L^2 T}$)
$q''_{U.eq}$: uniform equivalent heat flux ($\frac{E}{L^2 T}$)
$\overline{q''}_{N.U}$: average non uniform flux ($\frac{E}{L^2 T}$)
q''_{DNBU}	: critical uniform heat flux ($\frac{E}{L^2 T}$)
Q_L	: volume of liquid crossing the lower surface of the bubbly layer per unit time and area (L/T)
Q_F	: liquid peripheral film flow rate in annular flow regime (L/LT)
R	: rate of droplet deposition ($\frac{M}{L^2 T}$)
s	: thickness of superheated layer (L)
t	: thickness of liquid layer in annular flow regime (L)
T	: temperature (T)
T_W	: heater surface temperature (T)
T_{SAT}	: temperature of saturated liquid or of the bubble layer (T)
T_{SURR}	: temperature of superheated layer (T)
T_{JL}	: temperature difference defined by Jens and Lottes equation (T)
T_{BL}	: temperature of bubble detachment (T)
T_{d1}	: temperature of inception of bubble detached boiling calculate with equation (v) (T)
T_{d2}	: temperature of inception of bubble detached boiling calculate with equation (z) (T)
U^*	: critical relative velocity between liquid and bubbles ($\frac{L}{T}$)
V	: velocity ($\frac{L}{T}$)
V_{in}	: inlet velocity (L/T)

V_L : velocity of the liquid across the bubbly layer (L/T)
 v_g : specific volume of steam (L^3/M)
 W : liquid film flow rate in annular regime ($\frac{M}{L^2 T}$)
 W_0 : liquid film flow rate at annular flow onset ($\frac{M}{L^2 T}$)
 Z : distance in the direction of flow (L)

α : void fraction (-)
 δ : proportionality constant (-)
 ϵ : porosity of the bubble layer (-)
 μ : dynamic viscosity ($\frac{M}{T L}$)
 ρ : density (M/L^3)
 ρ_L : density of liquid crossing the bubble layer (M/L^3)
 σ : surface tension (F/L)

1. INTRODUCTION (*)

In nuclear reactor core thermal design only non-uniform axial heating must be considered. The shape of the heat flux distribution varies over the core lifetime; therefore it is very important to be able to correctly predict the effect of non-uniform axial flux distribution on DNB.

Recent tests conducted by various laboratories (1) (2) (3) (4) (5) have shown a marked influence of the heat flux distribution both on DNB power and location point.

A correction factor, derived by a theoretical analysis, has been proposed in order to predict non uniform heat flux DNB conditions from corresponding uniform flux data (5) (6).

Scope of the present work is to define the field of applicability of the theoretical approach reported on references (5) and (6) to point out the role of some important parameter such DNB length and pressure and to modify the theoretical analysis for the high quality region.

An analytical expression for factor $C = \frac{h}{\rho V_s C_p}$ in bubbly flow region has been derived.

(*) Manuscript received on July 1966

2. THEORETICAL ANALYSIS

Knowledge of the flow regime existing in a heated channel is necessary for true evaluation of the heat transfer process. The following theoretical analysis covers bubbly and annular dispersed flow regions that are of prime interest for water reactors design.

2.a - BUBBLY FLOW

This region should cover both subcooled and low qualities boiling. With high heat fluxes local boiling occurs before the average enthalpy of the fluid has reached the saturation value. Therefore a flow characterized by a continuous liquid phase with small bubbles exist over a given length of the heated channel before the saturation point.

In the bubbly flow region DNB occurrence can be postulated as an overheating of the power generating surface after the superheat degree of the adjacent liquid layer has reached a critical value. Therefore the past history of superheated liquid layer up to DNB point is important to define critical conditions.

In reference (6) it is proposed a physical model where a bubbly layer of tiny bubbles separates the main stream from the superheated liquid layer near the wall where bubbles nucleate and grow (Fig.1). This model seems justified from experimental evidence. Nevstrueva and Gonzales (7) have verified by β ray absorption that dispersed flow is present in layers close to the heated wall and compact subcooled liquid flows undisturbed farther from the heater. Tippetts (8), for the subcooled region reports that vapor bubbles slide along the heated surface at a velocity lower than the mean channel velocity in an irregular frothy layer of liquid and bubbles. It was found that the bubbles do not remain always attached to the heated wall.

Similar conclusion can be drawn from photographic studies conducted both in England and USA on Freon 113.

The energy balance of the superheated layer should yield the critical enthalpy value for the onset of DNB.

Tong (6) writes the energy equation for the superheated layer as follows :

$$\frac{d}{dz} (\rho V P s H_z) + \frac{hP}{C_p} (H_z - H_{SAT}) = q'' P \quad (a)$$

To solve equation (a) the following assumptions are made :

- 1) Physical properties of the superheated liquid layer are independent of position.
- 2) Thickness and average velocity of the superheated layer are constant.
- 3) The specific heat of the superheated layer is equal to that of saturated liquid.
- 4) The temperature at the lower side of the bubble layer is the saturation temperature and therefore constant.
- 5) The heat transfer coefficient h from superheated layer to bubbly layer is constant.

Therefore equation (a) can be written as follows :

$$\frac{d(H_z - H_{SAT})}{dz} + C(H_z - H_{SAT}) = C \frac{C_p}{h} q'' \quad (b)$$

where $C = \frac{h}{\rho V s C_p}$

In reference (6) equation (b) is solved using the initial condition $H(0) - H_{SAT} = 0$; that is the energy balance is taken from the inception of local boiling.

Postulating that the critical enthalpy of the superheated layer is the same for both uniform and non uniform heat flux distribution having same local conditions we can write

$$(H_{DNB} - H_{SAT})_{UNFLUX} = (H_{DNB} - H_{SAT})_{NUNFLUX} \quad (c)$$

Solving equation (b) up to the DNB location for both uniform and non uniform heat flux distribution is therefore:

$$q''_{DNB U} (1 - e^{-C l_{DNB U}}) = C \int_0^{l_{DNB NU}} q''(z) \cdot e^{-C (l_{DNB NU} - z)} dz \quad (d)$$

When $l_{DNB U}$ and $l_{DNB NU}$ are the DNB locations for uniform and non uniform heat flux distribution measured from local boiling inception.

Now a correction factor F that multiplied by the non uniform local DNB heat flux yields the uniform equivalent heat flux can be defined as :

$$F = \frac{C \int_0^{l_{DNB NU}} q''(z) e^{-C (l_{DNB NU} - z)} dz}{q''_{DNB loc} \cdot (1 - e^{-C l_{DNB U}})} \quad (e)$$

The value of factor C given in Ref. (6) (called here after C_t), as

$$C_t = 805,843 \frac{(1 - x)^{7,9}}{G^{1,72}} \quad \begin{matrix} C_t \text{ in } \text{cm}^{-1} \\ G \text{ in } \frac{\text{g}}{\text{cm}^2 \text{ s}} \end{matrix} \quad (f)$$

has been determined empirically using equation (d). However the DNB length, l_{DNB} , was taken from test section inlet rather than from local boiling inception.

This analysis, reported from ref.(6) has been proposed valid for a wide range of quality ($- 0,25 < X < 0,75$) covering certainly also annular flow region. In the following paragraphs a new expression for C , derived theoretically is given and is investigated the role of the DNB length in correctly define factor F . The analysis is also extended to the annular flow region for which a new expression of $C = C_a$ is proposed.

2.a.1 - Theoretical evaluation of factor C for bubbly flow regime

In reference (6) no attempt has been made to derive an analytical expression of the factor $C = \frac{h}{\rho V_s C_p}$

However it is possible to obtain theoretically the dependence of C from the important parameters X, T_{SAT} and G; the unknown proportionality factor can be obtained only empirically from equation (d).

This can be accomplished considering one by one the various component of C expression :

a) Heat transfer coefficient "h".

This coefficient has been defined as the heat transfer coefficient between the superheated layer and the bubbly layer. Actually h represents a fictitious heat transfer coefficient since the heat is not removed by convection.

Considering the physical model of Fig.1 it can be assumed that when the bubbles that nucleate and grow in the superheated liquid layer detach from the wall, a pumping of water through the bubbly bed takes place for continuity reasons.

The water, having an initial enthalpy close to saturation, takes the place of the leaving bubbles and heats up to the local superheated enthalpy.

The same volume of superheated liquid is pushed by the growing bubbles from the liquid layer close to the heated surface into the cold region.

Since no exact esteem of vapour volume disappeared per unit area and time from the superheated liquid layer is possible, a proportionality criterion must be used.

We can write

$$q_t'' = h \cdot (T_{SURR} - T_{SAT}) = C_{pL} (T_{SURR} - T_{SAT}) Q_L \rho_L \quad (g)$$

where Q_L represents the liquid volume crossing the lower surface of the bubbly layer per unit time and area.

This volume $Q_L = (1 - \alpha) V_L$ is proportional to the contact area free of bubbles $(1 - \alpha)$ existing at the boundary between superheated and bubbly layer and inversely proportional to the resistance experienced in crossing the bubbly layer $(\frac{1}{\Delta P_{bl}})$

By definition is :

$$Q_L = (1 - \alpha) V_L \quad (h)$$

where V_L = velocity of the liquid crossing the bubbly layer radially.

The bubbly layer has concentration of small bubbles proportional to the void fraction α and can be considered, as far as pressure drop is concerned as a packed bed of porosity $\epsilon = 1 - \alpha$. After Ergun (9) the pressure drop for liquid in laminar motion through a packed bed is :

$$\Delta P_{bl} = \Delta P_{PB} \approx V_L \cdot \frac{(1 - \epsilon)^2}{\epsilon^3} = V_L \frac{\alpha^2}{(1 - \alpha)^3} \quad (i)$$

Since $Q_L \approx \frac{1}{\Delta P_{PB}}$ we can write :

$$(1 - \alpha) V_L \approx \frac{(1 - \alpha)^3}{V_L \alpha^2} \quad (1) \quad \text{or} \quad V_L = K \frac{(1 - \alpha)}{\alpha} \quad (m)$$

substituting (m) in (h) we obtain

$$Q_L = K \frac{(1 - \alpha)^2}{\alpha} \quad (n)$$

To correlate void fraction with local quality X , the Martinelli-Nelson method has been used. The values obtained for $R = \frac{(1 - \alpha)^2}{\alpha}$ at 70 and 140 ata have been plotted on a log-log paper versus $1 - X$.

The general relation-ship obtained is $R \approx (1 - x)^a$ and the resulting values of exponent "a" are in the following table :

p = 140 ata	p = 70 ata
6,54	6,105 for $0,1 < X < 0,3$
2,71	2,6 " $0,4 < X < 0,7$
2,32	2,25 " $0,8 < X < 0,9$

It should be pointed out that the low values of exponent "a" are not to be considered as reliable. In fact the analysis here applied is valid only in the bubble flow region. For $X < 0,1$ and in the subcooled void region the value of exponent "a" is close to the one for $0,1 < X < 0,3$ for the slope of the detached void vs. quality does not vary sensibly from that in higher quality region.

It can be concluded that for the field of interest, exponent "a" is a weak function of pressure and quality.

Since the liquid that replaces the detached bubbles has to be diverted from the axially flowing liquid core, the inertia of the main stream will act to increase the lateral resistance.

In reference (10) is reported that the increase in lateral resistance expressed as K/K_∞ becomes very large when $\Delta P/G^2$ is less than 0,1 for a wide range of geometries. The proposed correlation is $K/K_\infty \approx \left(\frac{\Delta P_L}{G^2}\right)^{-1}$; therefore the lateral pressure drop will increase proportional

ly to the axial mass velocity G_a .

Extrapolation of this result to the present case may not be entirely correct; however a reduction of h and therefore of C should be found as G increases.

Equation (n) may now be rewritten as

$$h = K_1 \frac{C_{PL} \cdot g_L}{G} (1 - x)^a \quad (o)$$

where $a = a(X, T_{SAT})$

For the pressure range investigated ($70 < p < 140$ ata) the suggested value for exponent "a" varies from 6,5 to 6,1.

b) Velocity of superheated liquid layer V.

The bubbly layer established at high flow rates covering the superheated liquid contains a high concentration of small bubbles. In this conditions the dynamic forces applied to the bubbles by the ambient liquid will be entirely of viscous nature. A critical relative velocity between liquid and bubbles is predicted by Chang (11) as $U^* = \frac{\sigma}{\mu}$. Hence the bubbly layer velocity approach a limit as the bulk flow velocity is continuously increased. Therefore also the shear of the bubbly layer on superheated liquid and the velocity of the outer portion of this layer reaches a limiting value. The average velocity of the superheated layer of constant thickness "s" (see subparagraph c) can be expressed as

$$V = K_2 \frac{\sigma}{\mu} \quad (p)$$

where σ and μ are both functions of T_{SAT} .

c) Thickness of liquid layer s.

From momentum equation applied to the superheated liquid layer, for specified fluid viscosity, boundary velocity shear and pressure gradient (reference 6, Appendix A) the thickness "s" of the liquid layer results constant. Tests on Freon have shown the presence of a liquid layer about 0,8 mm thick under the bubbly layer.

Introducing equation (o) and (p) in the expression $C = \frac{h}{\rho V s C_p}$

$$\text{we obtain } C = K_1 \frac{C_{pL} \rho_L}{G} \cdot \frac{(1-x)^2}{\rho_{SURR} \cdot K_2 \frac{\sigma}{\mu} \cdot s \cdot C_{pSURR}} \quad (q)$$

./.

It can be assumed $C_{PSURR} = C_{PL} = C_{PSAT}$ and $P_{SURR} = P_L = P_{SAT}$ without introducing large errors.

Hence

$$C = K_3 \frac{(1-x)^a}{G \cdot s \frac{\sigma}{\mu}} \quad (r)$$

or, recalling the constance of s ,

$$C = K \cdot \frac{(1-x)^a}{G \cdot f(T_{SAT})} \quad (s)$$

The value of the proportionality factor K has been obtained comparing DNB data of uniform and non uniform heat flux distribution having same local condition at DNB through equation (d). The value of K has been found to be almost a constant and equal to $3,6624 \times 10^{-2}$.

Therefore the proposed expression for C , here after called C_F is :

$$C_F = \frac{3,6624 \cdot 10^{-2}}{G \cdot f_1(T_{SAT})} (1-x)^a \quad \left[\text{cm}^{-1} \right] \quad (t)$$

where $a = 6,105 + 0,44 \cdot 10^{-3} (14,223 p - 1000)$

$$f_1(T_{SAT}) = 417,262384 \cdot 10^{-15} T_{SAT}^4 - 384,425667 \cdot 10^{-12} T_{SAT}^3 - 144,546819 \cdot 10^{-9} T_{SAT}^2 + 80,140495 \cdot 10^{-6} T_{SAT} - 0,476812 \cdot 10^{-3}$$

p = test pressure (ata)

T_{SAT} = saturation temperature ($^{\circ}\text{C}$)

G = mass velocity $\left(\frac{\text{g}}{\text{cm}^2 \text{ s}} \right)$

x = local quality at DNB location.

2.a.2 - Influence of DNB length on non uniform heat flux prediction
(bubble flow region).

The ability to reduce a non-uniform heat flux distribution to a uniform one as far as DNB prediction is concerned is particularly important when the two DNB powers are quite different. Otherwise the need to use a correction factor F as proposed in reference (6) is reduced since $q''_{ueq} \approx \bar{q}''_{NU}$ within a small percentual error.

The difference between critical powers for couples of experimental DNB points having similar value for local bulk conditions, namely X_{DNB} , De , p and G , varies essentially as function of X_{DNB} , pressure and non uniform heat flux distribution. For the couples taken from Reference (2), where the DNB location is very well defined, the two critical powers have been reported as function of X_{DNB} for constant G , p , De and heat flux distribution (Fig. 2, 3, 4, 5, 6).

The DNB length, l_{DNB} , measured from the inlet of test section is equal for high values of X_{DNB} (DNB occurs at section end); when the DNB location moves from the section exit toward the maximum heat flux location (for the non uniform power distribution) the two l_{DNB} become different.

A study was made in order to find out the influence of the length to be introduced as l_{DNB} in equations (d) and (e) i.e. of the length to be used in the energy balance of the superheated liquid layer.

Although in Reference (6) not a great importance has been given to this point it will be shown later in the paper that different DNB length will lead in practice to quite different results and errors can from it arise in predicting equivalent uniform DNB fluxes.

In reference (6) it is suggested to measure the DNB length (l_{DNB}) from the inception of local boiling; however to evaluate the expression of C and to check the prediction of the proposed method the DNB length, l_{DNB} , was taken from test section inlet rather than

from the inception of local boiling. Two justifications have been brought for this decision, i.e. the fact that local boiling usually occurs very near the inlet of a test section in DNB conditions and the postulated rapid decay of the memory effect with distance.

Usually the onset of subcooled boiling is determined by the Jens & Lottes relation $T_{JL} = T_W - T_{SAT} = 7,92 (q'')^{1/4} e^{-\frac{p}{63,278}}$

$$T_{JL} (^{\circ}C) ; q'' (W/cm^2) ; p (ata)$$

that fixes the shape of q'' vs. $T_W - T_{SAT}$ in the region where the influence of mass flow rate and subcooling is vanished (Fig. 7). The temperature where the condition for nucleation is reached is defined as

$$T_{LB} = T_{SAT} + T_{JL} - \frac{q''}{h} \quad (u)$$

The intersection point between the two curves, that is fully developed nucleate boiling and forced convection, lies in the "partial boiling" region. Therefore a single phase heat transfer process, more or less important as function of subcooling degree, takes place between comparatively few nucleation sites.

This was also shown experimentally by Griffith, Clark and Rosenhaw (12) that observed the bubbles appear on the heated surface in strands with a width approximately equal to the height.

Therefore the length from which start the energy balance of superheated layer can not be taken as the local boiling onset length defined above.

Two other points can be considered as initial length for the energy balance, i.e. the fully developed nucleate boiling point and the bubble detachment point. Actually only the latter is consistent with the physical model adopted (Fig.1). In fact at the upper limit of the wall voidage region not a bubbly layer on top of a superheated liquid layer has build up, but are present bubbles of limited dimensions ($0,07 \pm 0,1$ mm, ref.13) within the superheated layer. Experiments have shown that the slightly subcooled region or detached

void region starts for wall voidage thickness of about 0,1 mm, that is of the size of the bubbles.

The transition point between the wall and detached boiling region has been evaluated using two different criterion :

$$T_{d1} = T_{SAT} - q''/5h \quad (\text{as per Reference 12}) \quad (v)$$

$$T_{d2} = T_{SAT} - q''\eta/V_{in} \quad (\text{as per Reference 13}) \quad (z)$$

It is hence made the assumption that the bubble detachment occurs at a length shorter than the DNB location. This assumption seems justified by the following considerations. In the bubbly flow region, at the critical condition the bubble on the heated surface has developed to its final size under hydrodynamic and thermodynamic equilibrium. In the case of saturated boiling this statement is obvious.

In the range of nucleate boiling of subcooled liquid, the bubbles at the DNB condition should be, at least, about to detach from the heated surface. In fact, if the bubbles collapse on the heater it means that the liquid layer adjacent to the wall can sustain more superheat and therefore the heat flux would not be the maximum. However at very high subcooling it may happen that the bubble detachment point, evaluated by both equation (v) and (z), falls behind DNB locations (l_{DNB}) for a few cases obtained from Reference 2.

Further theoretical and experimental work on this point is required in order to avoid any possible error introduced by uncorrect bubble detachment point evaluation.

Several pairs of experimental DNB data points, a non uniform-flux point and a corresponding uniform flux point were selected from Reference 2.

The shapes of flux distribution considered included simmetrical cosine, peak skewed toward the top and toward the bottom (Fig. 8). Each pair had similar values for local conditions, i.e. :

X_{DNB} , De , p and G . The DNB length, l_{DNB} , to be introduced in equation (e) in order to evaluate the factor $C = \frac{h}{9VSC_p}$ was measured from the following locations:

- Case I-a-1 Inlet of test section (as in Reference 6)
- Case I-a-2 Onset of bubbles detachment as evaluated according to equation (v)
- Case I-a-3 Onset of bubbles detachment as evaluated according to equation (z).

The important data of the selected pairs are reported in Table 1.

The results obtained for the factor $F = \frac{q''_{DNB \text{ uniform flux}}}{q''_{DNB \text{ local in non uniform flux}}}$ are given in Table 2.

The calculations have been performed through equation (d) by using both the method presented in Reference (6) (that is l_{DNB} measured from test section inlet and $C = C_t$) and the method outlined above (that is l_{DNB} measured from bubble detachment onset and $C = C_F$). Since the method of Reference (6) calls for DNB length equal in the uniform and non uniform heat flux condition, theoretical critical power evaluated through the W3 correlation has also been considered for a uniform DNB length equal to the non uniform one in the cases when the DNB location (for the non uniform heat flux distribution) is not at channel exit (Table 2).

The results have also been plotted as $F_{measured}$ vs. $F_{predicted}$ in Fig.9, 10 and 11.

In order to check the prediction of the uniform equivalent critical heat flux obtained through the method outlined in the present paper for couples taken from sources other than Reference (2) and not used to find C_F empirical constant, the cosine distribution and uniform heat flux given in Ref.3 have been selected. The results, plotted as $F_{measured}$ vs. $F_{predicted}$ are given in Fig.12.

The calculations have also been performed with the method of Ref.(6) and similarly plotted in Fig.13. Among the possible couples given in Ref.3, only those with very high DNB quality have not been used

for comparison since this is made in Section 2b (Annular flow region).

The results obtained give confidence in using both the method and the C_p expression proposed in the present paper in order to find, with minimum error, the equivalent uniform DNB heat flux or the correction factor F .

2.b - ANNULAR FLOW

The characteristics of an annular flow (Fig.14) boiling crisis is a discontinuity of the liquid film near the wall. Vanderwater (14) has suggested that the thickness of the liquid film depends on the balance of the liquid droplet deposition rate, the liquid evaporation rate and the liquid re-entrainment rate.

Quandt (15) found that the net mass exchange rate from the liquid film, due to entrainment and droplet diffusion is linearly related with peripheral film flow rate $Q_f = \rho_l t V_f$

Although this result was obtained in an isothermal annular flow, it can be assumed that a similar relation-ship should held also for non adiabatic steam-water flow.

In Reference (5) it is shown that the net droplet diffusion and re-entrainment rate of liquid flow to the film is :

$$R-E = \frac{C'}{D} (W_o - W) \quad (1a)$$

$$\text{where } C' = \frac{K_1 G^{n-1}}{XVg} + K_2 D \quad (2a)$$

and W_o "would represent the equilibrium film flow rate for developed flow at a particular quality if the channel had no further heat input" (quote from Ref. 5).

A mass balance of the film can be written as :

$$\frac{dW}{dz} = R-E - \frac{q''}{H_{fg}} \quad (3a)$$

or, substituting (1a) for R-E

$$\frac{dW}{dz} = \frac{C'}{D} (W_0 - W) - \frac{q''}{H_{fg}} \quad (4a)$$

$$\text{Calling } \frac{C'}{D} = Ca = \frac{K_1 G^{n-1}}{X V_g D} + K_2 \quad (5a)$$

equation (4a) becomes :

$$\frac{d(W_0 - W)}{dz} + Ca (W_0 - W) = \frac{q''}{H_{fg}} \quad (6a)$$

Assuming Ca to be a weak function of length the general solution of equation (6a) is :

$$W_0 - W = e^{-Ca z} \left(K - \int \frac{q''(z)}{H_{fg}} e^{Ca z} dz \right) \quad (7a)$$

Solving equation (7a) for the case of uniform heat flux and using the boundary condition $(W)_{z=0} = W_0$ (W_0 is the flow rate of the liquid film at annular flow onset) we obtain

$$W_0 - W(z) = \frac{q''}{Ca H_{fg}} (1 - e^{-Ca z}) \quad (8a)$$

where z = distance from inception of annular flow.

Equation (8a) is formally identical to the first member of equation (d) obtained in section 2a although the physical meaning is entirely different. In fact in section 2a was used an energy balance to predict burnout while here a mass balance was used.

Similarly to section 2a a correction factor

$$F_a = \frac{q''_{DNB, \text{ equivalent to uniform flux}}}{q''_{DNB, \text{ local in non-uniform flux}}}$$

can be developed assuming that the critical value of $W_0 - W$ would occur for both uniform and non uniform flux at the same local quality.

It can be therefore written :

$$q''_{DNBU} (1 - e^{-Ca L_{aDNB}}) = Ca \int_0^{L_{aDNB}} q''(z) e^{-Ca (L_{aDNB} - z)} dz \quad (9a)$$

where L_a DNB and l_a DNB represents the annular flow length in uniform and non uniform heat flux distribution up to the DNB point (DNB length). A similar analitical derivation is reported in Ref. (5); however the DNB length is taken from channel inlet, although for all the cases tested inlet enthalpy is subcooled and the integration is made with z/D as variable.

Several pairs of experimental DNB data points with high burnout quality having similar values for local conditions have been selected both to find through equation (9a) the value of the factor C_a and to check the influence of the DNB length (Table 3).

An expression for C_a , derived from equation (5a) assuming K_2 negligible compared with $\frac{K_1 G^{n-1}}{X VgD}$ has been obtained as :

$$C_a = \frac{95,573}{X \cdot Vg \cdot D \cdot G^{1,5}} \quad (10a)$$

where D : equivalent diameter (cm)

G : mass velocity (g/cm^2s)

X : quality

Vg : steam specific volume (cm^3/g)

Applying this C_a expression to all the couples reported in Table 3 the correction factor $F_a = \frac{q''_{DNB, \text{ equivalent to uniform flux}}}{q''_{DNB, \text{ local in non-uniform flux}}}$ has been derived (Table 4).

The following cases have been considered :

2b-1) $P = 36,209 \text{ ata}$

From Reference (5) nine couples have been selected with five different non uniform heat flux distribution. The important data are reported in Table 3 while the non-uniform distribution are represented in Fig.15. For all the couples calculations have been performed using, for comparison, different methods; the DNB length has been taken both from inlet (Ref.5 method) and from annular flow onset (proposed method). In order to avoid possible errors arising in defining the beginning of annular flow, experimental results on

heated channel two phase flow regime reported in Reference (16) for the same pressure, length, flow rate and similar diameter have been used. The results obtained, reported as F_{measured} versus $F_{\text{predicted}}$ are plotted in Fig.17 and 19.

For a few cases the calculations have been performed using Ref.5 method introducing a C value derived from equation (f). The results are reported in Table 4 and Fig.18.

2b-2) $P = 70,309 \text{ ata}$

Four couples have been selected from Reference (3) and one from reference (17); the calculations have been performed by all methods previously described. The important data are in Table 3 and the non uniform power distribution in Fig.16.

The results obtained are reported in Figg. 17, 18 and 19. The annular flow onset length has been taken from experimental results reported on reference 16.

The important conclusion is similar to that of Section 2a i.e. the influence of DNB length is small if the DNB power of uniform and non uniform test sections are comparable. As the two critical powers becomes more and more different (function of non-uniform flux shape, pressure, test section length, ecc.) the error introduced taking the DNB length from test section inlet becomes larger and larger.

The results obtained from 36,2 and 70,3 ata points show that both the method and the C_a expression here proposed could be usefully used in the high quality region to find out an equivalent uniform DNB flux. However the promising results here obtained should be checked on a larger number of cases and it is well possible that the C_a expression will require some adjustment. Furthermore the uncertainty of the bubble flow regime boundary can lead to some error. We hope that the difficulty to correctly define the annular flow onset will be in the next future overcome since a great deal of work is presently devoted by several Laboratories to study two phase flow regimes in non adiabatic conditions.

ACKNOWLEDGEMENTS

The authors wishes to thank Messrs A.MOLINO, R.RICCARDI and
A.VALTANCOLI who performed the sometime tiresome calculations with
care and endurance and prepared many of the figures of this report.

* * *

REFERENCES

- 1) LEE, D.H. and OBERTELLI, J.D. - "An experimental investigation of forced convection burnout in high pressure water. Part. II - Preliminary results for Round Tubes with non-uniform axial heat flux distribution" AEEW-R-309-Winfrith, England 1963.
- 2) F.BIANCONE, A.CAMPANILE, G.GALIMI and M.GOFFI - "Forced convection burnout and hydrodynamic instability experiments for water at high pressure Part 1 : Presentation of data for round tubes with uniform power distribution" EUR 2490.e (1965).
- 3) Indd, D.F. et al. - "Non uniform heat generation experimental program" BAW - 3238-5 (1964)
- 4) STEVENS, G.F., ELLIOT, D.F. and WOOD R.W. - "An experimental comparison between forced convection burnout in Freon 12 flowing vertically upwards through uniformly and non-uniformly heated round tubes" AEEW-R-426 (1965).
- 5) SMITH, O.G. - "Non uniform heat flux burnout in vertical circular tubes with up-ward water flow" WCAP-2795 (1965).
- 6) L.S. TONG et al. - "Influence of axially non-uniform heat flux on DNB" WCAP - 2767 (1965).
- 7) NEVSTRUEVA, E.I. and GONZALES, J. - "Measurement of steam distribution by β -ray absorption in conditions of local boiling" Teploemergetike, (September 1960.)
- 8) TIPPETS, E.E. - "Critical heat fluxes and flow patterns in high pressure boiling water flows" -ASME Paper no.62-WA-162 (1962).
- 9) LAPIDES, N.E. and BRUBAKER, R.C. - "Source book for flow through packed beds" - G.E. Do 54-1-75 (1954).
- 10) BERNINGER, R.T., PREVITI, G. and L.S. TONG - "The hydraulic design of a model to simulate on open lattice PWR core" WCAP-1783 (1961).
- 11) CHANG, Y.P. - "An analysis of the critical conditions and burnout in boiling heat transfer" TID-14004 (1961).
- 12) GRIFFITH, P., CLARK, M.A. and ROHSENOV, W.M. - "Void volumes in sub-cooled boiling systems" - ASME paper no. 58-HT-19 (1958).
- 13) BOWRING, R.W. - "Physical model, based on bubble detachment, and calculation of steam voidage in the subcooled region of a heated channel" - HPR-10 (1962).

- 14) VANDERWATER, R.G. - "An analysis of burnout in two-phase, liquid-vapor flow" Ph. D. Thesis, University of Minnesota (1956).
- 15) QUANDT, E. - "Measurement of some basic parameters in two-phase annular flow" - AIChE Annual Meeting, P.Chicago (1962) - Preprint no. 36.
- 16) BERGLES, A.E. et al. "Investigation of boiling flow regimes and critical heat flux" - NYD - 3304 - 5 (1965)
- 17) BERTOLETTI, S. et al. "Critical heat flux data for fully developed flow of steam - water mixtures in round vertical tubes with non uniform axial power distribution "CISE - R 70 (1963)
- 18) BAKER, O. "Simultaneous flow of oil and gas" - Oil and Gas Journal 53, 185 - 190 (1954).

TABLE N° 1 DATA

Ref.2 -REPORT T/353 SORIN <div> Axial flux distribution : uniform-test section n° 1 Axial flux distribution : cosine-test section n° 2 </div>										
COUPLE'S NUMBER	RUN'S NUMBER	PRESSURE ata	MASS FLOW RATE g/cm s	INLET SUB- COOLING °C	TOTAL POWER (kW)	q'', q''_{\max} W/cm ²	QUALITY x_{DNB} (%)	(Z/L) DNB	(Z/L) BUBBLE (+) DETACHEMENT POINT (MIT)	(Z/L) BUBBLE (++) DETACHEMENT POINT (Bowring)
1 A	24 27/3/64	125,9	196,5	92,8	188	235,62	-6,63	1	0,90	0,75
	117 7/10/64	126,2	195,9	48	114	273,8	-6,00	0,735	0,55	0,462
2 A	70 25/3/64	127,2	152,1	157,6	206	291,05	-16,59	1	-	0,9
	52 7/10/64	126,2	152,9	83,7	132	317,03	-16,7	0,621	-	0,512
3 A	138 23/3/64	141,2	152,9	9,7	67	94,66	11,19	1	0,05	0,0
	40 17/2/65	141,2	142,4	3,5	54	129,69	10,5	0,816	0,125	0,075
4 A	120 26/6/64	140,7	154,2	20,3	78,5	110,91	7,81	1	0,275	-
	188 16/2/65	141,7	142,9	12,1	64,5	154,92	7,98	0,773	0,25	-
5 A	114 26/3/64	140,7	152,9	37,9	97	137,05	3,61	1	0,525	-
	141 13/2/65	141,7	142,5	26,5	79,5	190,94	3,1	0,730	0,375	-

(+) Calculated with MIT bubble detachment temperature (T_{α}) equation: $T_{\alpha(i)} = T_{SAT} - \frac{\phi(i)}{5 \cdot h(i)}$ where $h(i) = 0,03 \frac{K}{De} (Re)^{0,8} (Pr)^{0,4}$

De = hydraulic diameter (m); K = thermal conductivity (kcal/h m °C); h = film heat transfer coefficient (kcal/h m² °C); $T_{\alpha(i)}$ = local water temperature (°C); $\phi(i)$ = local flux (kcal/h m²); T_{SAT} = saturation temperature (°C); Re = Reynold's number (-); Pr = Prandtl's number

(++) Calculated with Bowring bubble detachment temperature (T_{α}) equation:

$$T_{\alpha(i)} = T_{SAT} - \eta \frac{\phi(i)}{V_{IN}} \quad \text{where: } \eta = 0,20226 (0,93 + 0,006684 \cdot p)$$

V_{IN} = inlet velocity (m/h); T_{SAT} = saturation temperature (°C);

p = pressure (ata)

TABLE N° 1 CONT'D

Ref. 2 - REPORT T/363 SORIN { Axial flux distribution : uniform-test section n° 1C { Axial flux distribution : upward skewed asymmetrical sine-test section n° 2B										
COUPLE'S NUMBER	RUN'S NUMBER	PRESSURE ATA	MASS FLOW RATE $\frac{g}{cm^2 s}$	INLET SUB- COOLING °C	TOTAL POWER (kW)	\bar{q}'' , $\frac{1}{2}''$ $\frac{max}{2}$ W/cm	QUALITY X DNG (%)	(Z/L) DNG	(Z/L) BUBBLE (+) DETACHEMENT POINT (MIT)	(Z/L) BUBBLE (+ +) DETACHEMENT POINT (BORING)
1 B	110 2/3/65	131,3	185,6	20,5	57	132,17	13,85	1	0,225	-
	78 11-12-64	130,3	185	8,3	41	161,32	13,2	0,958	0,275	-
2 B	159 1/3/65	131	175,6	96,7	103,5	240	3,34	1	0,725	-
	113 11/12/64	131,3	179,9	51,6	66,5	232,14	2,35	0,868	0,55	-
3 B	131 2/3/65	130,7	229,0	21,9	63	146,09	10,49	1	0,30	-
	86 22/12/64	132,3	228,3	7,4	42,5	167,53	10,7	0,928	0,275	-
4 B	15 1/3/65	131,7	137,7	144,4	109,5	253,91	1,58	1	0,8	-
	121 10/12/64	131,3	141,3	61,3	60,5	238,49	1,32	0,838	0,575	-
5 B	93 2/3/65	131,3	140,3	20,5	52	120,58	19,12	1	0,20	-
	72 A 11/12/64	131,3	140,8	3,2	34	134,03	17,8	0,958	0,10	-
6 B	46 26/2/65	131,7	94,9	183,5	102	236,52	10,09	1	0,725	-
	41 22/12/64	131,3	94	60	54,5	214,85	10,5	0,808	0,462	-
7 B	141 2/3/65	131,3	314,2	21,1	75,25	174,49	7,98	1	0,35	-
	73 B 22/12/64	132,7	313	9,6	51,5	203,01	7,8	0,958	0,325	-

TABLE N° 1

CONT'D

Ref. 2 Report T/363 SORIN { Axial flux distribution : Uniform - Test Section n° 1C { Axial flux distribution : down skewed asymmetrical sine-test section n° 2C										
Couples NUMBER	RUN'S NUMBER	PRESSURE ata	MASS FLOW RATE g/cm sec	INLET SUB- COOLING °C	TOTAL POWER kW	q'', q''_{max} W/cm ²	QUALITY X _{DNB} (%)	(Z/L) _{DNB} —	(Z/L) BUBBLE (+) DETACHEMENT POINT (MIT)	(Z/L) BUBBLE (++) DETACHEMENT POINT (BOWRING)
1 C	110 2/3/65	131,3	185,6	20,5	57	132,17	13,85	1	0,225	—
	271 23/3/65	132,6	182,7	4,7	46	181,32	14,3	0,662	0,075	—
2 C	130 1/3/65	131,5	94,1	97,0	75	176,23	21,28	1	0,50	—
	180 23/3/65	132,3	95,6	11,5	40,5	159,65	21,2	0,603	0,10	—
3 C	141 2/3/65	131,3	314,2	21,1	75,25	174,49	7,98	1	0,35	—
	224 23/3/65	132,3	310,5	8,9	55,5	218,77	7,5	0,689	0,15	—
4 C	47 2/3/65	134,7	301	42,5	98,25	227,82	4,67	1	0,575	—
	160 23/3/65	132,3	306,2	15,2	61,7	243,22	5,1	0,631	0,20	—
5 C	104 26/2/65	132,3	185,1	198,8	166,25	385,51	-10,45	1	—	0,775
	182 22/3/65	131,7	182,1	98,5	99	390,25	-10,2	0,603	—	0,40

TABLE N° 1 CONT'D

Ref. 3-REPORT BABCOCK & WILCOX n° 7

{ Axial flux distribution : uniform
 { Axial flux distribution : chepped cosine

COUPLE'S NUMBER	RUN'S NUMBER	PRESSURE ATA	MASS FLOW RATE $\frac{2}{g/cm^3 s}$	H IN kcal/kg	TOTAL POWER (kW)	q'', q''_{max} $\frac{2}{W/cm}$	QUALITY X_{DNB} (%)	(Z/L) DNB —	(Z/L) BUBBLE (+) DETACHEMENT POINT (MIT)	(Z/L) BUBBLE (++) DETACHEMENT POINT (BOWRING)
1 D	71	105,1	202,91	264,5	103,1	158,51	14,8	1	0,50	-
	188	105,1	202,23	268,3	101,8	219,12	14,9	1	0,45	-
2 D	75	105,5	201,69	299,9	88	135,30	20,64	1	0,275	-
	185	105,5	203,73	324,2	73,2	157,56	20,35	0,875	0,175	-
3 D	78	105,7	332,31	299	100,2	154,05	9,95	1	0,45	-
	195	105,5	340,59	305	93,3	200,82	9,50	1	0,40	-
4 D	41	70,3	333,81	208,4	173,5	266,73	8,49	1	0,65	-
	171	71,7	342,35	237,4	141,8	305,22	8,84	1	0,50	-
5 D	32	70,7	338,42	236,2	155,2	238,62	12,05	1	0,475	-
	166	72,1	343,84	267,7	119,9	256,57	11,33	0,875	0,325	-
6 D	20	70,3	337,87	263,9	141,8	218,01	17,27	1	0,25	-
	165	71	339,64	289,9	115,3	248,18	17,38	0,875	0,1475	-

TABLE N° 2 RESULTS

Ref. 2: Report T/363 SURF $\left\{ \begin{array}{l} \text{axial flux distribution uniform-test section n° 1} \\ \text{axial flux distribution symmetrical cosine-test section n° 2} \end{array} \right.$								
COUPLE's NUMBER	C (Fiat) -1 cm	$\frac{F_{Meas}(Fiat)(1)}{F_{Pred}}$	$\frac{F_{Meas}(Fiat)(2)}{F_{Pred}}$	$\frac{F_{Meas}(Ref. 5)(5)}{F_{Pred}}$	C(Ref. 5) cm ⁻¹	$\frac{F_{Meas}}{F_{Pred}}(3)$	$\frac{F_{Meas}}{F_{Pred}}(4)$	$\frac{F_{Meas}}{F_{Pred}}(6)$
1 A	0,0962	1,015	-	1,235	0,1493	1,303	1,531	1,307
2 A	0,2326	-	0,975	0,983	0,4892	1,007	1,3107	1,007
3 A	0,0824	1,070	-	1,066	0,0605	1,092	1,217	1,091
4 A	0,0532	0,931	-	0,949	0,0758	0,981	1,125	0,98
5 A	0,0853	0,903	-	0,891	0,1124	0,921	1,075	0,921

(1) Obtained with Fiat method and MIT bubble detachment point

(2) Obtained with Fiat method and Bowring bubble detachment point

(3) Obtained with Ref. 6 method

(4) Obtained with Ref. 6 method and modified length

(5) Obtained with Fiat method and local boiling point

(6) Obtained with Ref. 6 method and local boiling point

TABLE N° 2 CONT'D

Ref. 2- REPORT T/363 SORIN <div> Axial flux distribution: uniform-test section n° 1 C Axial flux distribution: upward skewed asymmetrical sine-test section n° 2B </div>						
COUPLE'S NUMBER	$C(F_{iat})_{-1}$ cm	$\frac{F_{Meas}(F_{iat})(1)}{F_{Pred}}$	$\frac{F_{Meas}(F_{iat})(2)}{F_{Pred}}$	$C(Ref.6)_{-1}$ cm	$\frac{F_{Meas}}{F_{Pred}} (3)$	$\frac{F_{Meas}}{F_{Pred}} (4)$
1 B	0,0279	1,15	-	0,0381	1,17	1,20
2 B	0,0584	1,03	-	0,0574	1,1	1,17
3 B	0,0295	1,14	-	0,0295	1,182	1,24
4 B	0,0912	1,13	-	0,1433	1,264	1,369
5 B	0,0268	1,24	-	0,0337	1,3	1,336
6 B	0,0705	1,15	-	0,1372	1,227	1,38
7 B	0,0246	1,15	-	0,0171	1,23	1,275

TABLE N° 2 CONT'D

Ref.2 - Report T/363 BORIN <div> Axial flux distribution: uniform - test section n° 1C Axial flux distribution: down skewed asymmetrical sine-test section n° 2C </div>						
Couple's Number	$C_{(FIAT)} \text{ cm}^{-1}$	$\frac{F_{Meas}(FIAT) (1)}{F_{Pred}}$	$\frac{F_{Meas}(FIAT) (2)}{F_{Pred}}$	$C_{(Ref.6)} \text{ cm}^{-1}$	$\frac{F_{Meas} (3)}{F_{Pred}}$	$\frac{F_{Meas} (4)}{F_{Pred}}$
1 C	0,0262	0,98	-	0,0321	0,99	1,135
2 C	0,0308	1,27	-	0,0482	1,35	1,686
3 C	0,0249	1,075	-	0,0217	1,156	1,192
4 C	0,0314	1,09	-	0,0292	1,452	1,79
5 C	0,1427	-	1,29	0,2254	1,315	1,68

Ref. 3 - Report Babcock & Wilcox n° 7 <div> Axial flux distribution : uniform Axial flux distribution: cosine </div>						
Couple's Number	$C_{(FIAT)} \text{ cm}^{-1}$	$\frac{F_{Meas}(FIAT) (1)}{F_{Pred}}$	$\frac{F_{Meas}(FIAT) (2)}{F_{Pred}}$	$C_{(Ref.6)} \text{ cm}^{-1}$	$\frac{F_{Meas} (3)}{F_{Pred}}$	$\frac{F_{Meas} (4)}{F_{Pred}}$
1 D	0,0174	1,123	-	0,0243	1,211	-
3 D	0,015	1,148	-	0,0164	1,185	-
4 D	0,0118	1,095	-	0,018	1,389	-
5 D	0,0094	1,073	-	0,0148	1,16	1,241
6 D	0,0066	1,073	-	0,0082	1,207	1,231

TABLE N° 3 DATA

COUPLE'S NUMBER	RUN'S NUMBER	PRESSURE ATA	MASS FLOW RATE $\frac{2}{g/cm^2 s}$	H IN kcal/kg	TOTAL POWER (kW)	\bar{q}'' , q''_{max} $\frac{2}{W/cm^2}$	QUALITY X DNB (%)	QUALITY ONSET ANNULAR REGION %	AXIAL FLUX DISTRIBUTION		
1	Ref. 3	23	69,9	69,58	260,8	93,4	143,6	77,09	20	Babcock & Wilcox	uniform
		163	70,7	68,63	284,5	86,2	185,54	77,15	20	" " "	cosine
2	Ref. 3	18	70,3	207,25	267,8	129,8	199,57	31,97	19	" " "	uniform
		224	70,7	203,32	289,6	111,2	239,35	32,32	19	" " "	cosine
3	Ref. 3	81	105,6	36,90	318,7	58	89,17	57,91	17	" " "	uniform
		192	106	67,28	297,9	63,4	136,46	58,1	17	" " "	cosine
4	Ref. 3	12	70,3	204,00	287,8	119,9	164,34	34,96	19	" " "	uniform
		164	71	200,34	287,8	112,2	241,51	32,73	19	" " "	cosine
5	Ref. 5	A-25	36,2	149,20	295,5	-	519,14	42,6	6	WCAP-2795	uniform
		C-14	36,2	149,20	202,8	-	$q''C=643,56$ $q''2=100,61$	42,5	6	" "	non unif.
6	Ref. 5	A-26	36,2	149,20	145	-	559,83	34	6	" "	uniform
		B-41	36,2	149,20	202,8	-	$q''C=593,26$ $q''2=155,81$	33,6	6	" "	non unif.
7	Ref. 5	A-27	36,2	149,20	122,2	-	570,87	29,88	6	" "	uniform
		B-30	36,2	149,20	141,7	-	$q''C=599,25$ $q''2=323,28$	29,75	6	" "	non unif.
8	Ref. 5	A-16	36,2	149,20	141,7	-	336,17	39,8	6	" "	uniform
		C-17	36,2	149,20	169,4	-	$q''C=708,38$ $q''2=115,75$	39,8	6	" "	non unif.

TABLE N° 3 CONT'D

COUPLE'S NUMBER	RUN'S NUMBER	PRESSURE ata	MASS FLOW RATE $\frac{2}{g/cm^2 s}$	H_{IN} kcal/kg	TOTAL POWER (kW)	\bar{q}'' , q''_{max} $\frac{2}{W/cm}$	QUALITY X_{DNB} (%)	QUALITY ONSET ANNULAR REGION %	AXIAL FLUX DISTRIBUTION
9	Ref. 5 A-12	36,2	74,60	81,1	-	478,46	61,93	12,8	WCAP-2795: uniform
	G - 5	36,2	74,60	81,1	-	$q''_C = 496,43$ $q''_2 = 110,39$	62,86	12,8	" " non uniform
10	Ref. 5 A - 12	36,2	74,60	81,1	-	478,46	61,93	12,8	" " uniform
	G - 4	36,2	74,60	94,4	-	$q''_C = 480,98$ $q''_2 = 145,40$	62,86	12,8	" " non uniform
11	Ref. 5 A - 9	36,2	74,60	97,8	-	470,25	64,4	12,8	" " uniform
	B - 3	36,2	74,60	112,2	-	$q''_C = 477,83$ $q''_2 = 315,40$	64,24	12,8	" " non uniform
12	Ref. 5 A - 4	36,2	74,60	66,1	-	451,02	66,4	12,8	" " uniform
	C - 12	36,2	74,60	80	-	$q''_C = 548,47$ $q''_2 = 275,97$	66,9	12,8	" " non uniform
13	Ref. 5 A - 1	36,2	74,60	141,7	-	421,68	77,2	12,8	" " uniform
	E - 3	36,2	74,60	197,2	-	$q''_C = 468,36$ $q''_2 = 72,54$	77,2	12,8	" " non uniform
14	Ref. 17 1228	70,3	109,59	296,2	-	240,57	45,25	16	CISE R74 uniform
	0218	70,3	103,35	298,4	-	245,90	46,76	16	" " non uniform

TABLE N° 4 RESULTS-ANNULAR REGION

Couple's Number	$C_{(FIAT)} \text{ cm}^{-1}$	$\frac{F_{Meas}}{F_{Pred}} (FIAT)$	$C_{(Ref.6)} \text{ cm}^{-1}$	$\frac{F_{Meas}(Ref.6)}{F_{Pred}}$	$C_{(Ref.5)} \text{ cm}^{-1}$	$\frac{F_{Meas}}{F_{Pred}} (Ref.5)$
1	0,007	1,06	$0,0095 \times 10^{-4}$	1,13	0,0044	1,11
2	0,0032	1,00	0,0041	1,194	0,0044	1,19
3	0,0155	1,07	0,00078	0,965	0,0044	0,93
4	0,0030	0,995	0,0032	1,095	0,0044	1,09
5	0,0037	1,027	-	-	0,0044	1,06
6	0,0048	1,01	-	-	0,0044	0,975
7	0,0055	1,006	-	-	0,0044	0,968
8	0,0041	1,016	0,0026 (+)	1,114	0,0044	0,992
9	0,0074	0,961	-	-	0,0044	0,961
10	0,0075	0,935	-	-	0,0044	0,991
11	0,0072	1,019	-	-	0,0044	0,987
12	0,0077	0,999	0,00009(+)	1,018	0,0044	0,991
13	0,0060	1,018	$0,39 \times 10^{-5}$ (+)	1,149	0,0044	0,923
14	0,0062	0,92	0,0019	0,98	-	-

(+) Extrapolated values from equation (f)

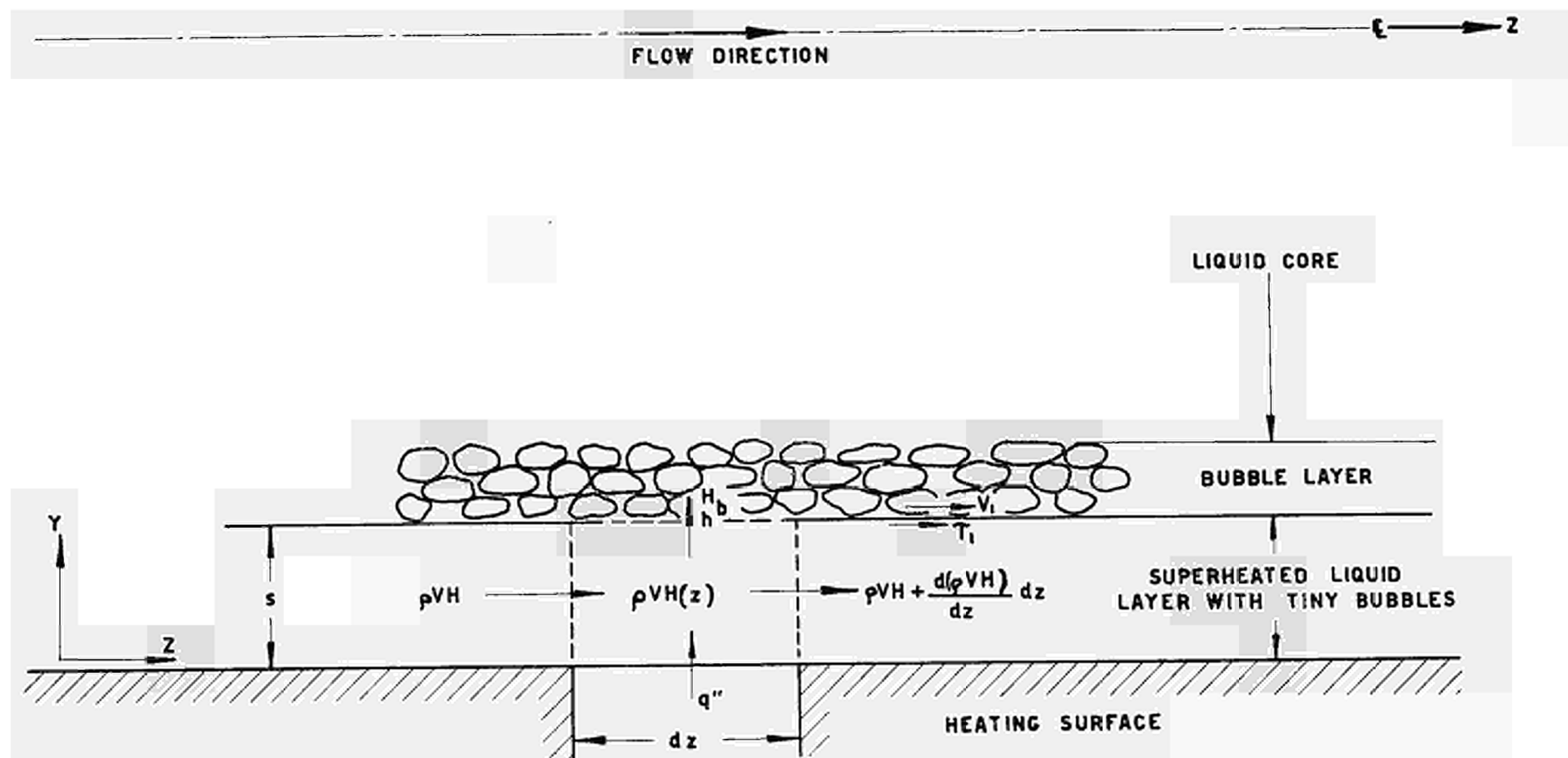


FIG. 1.

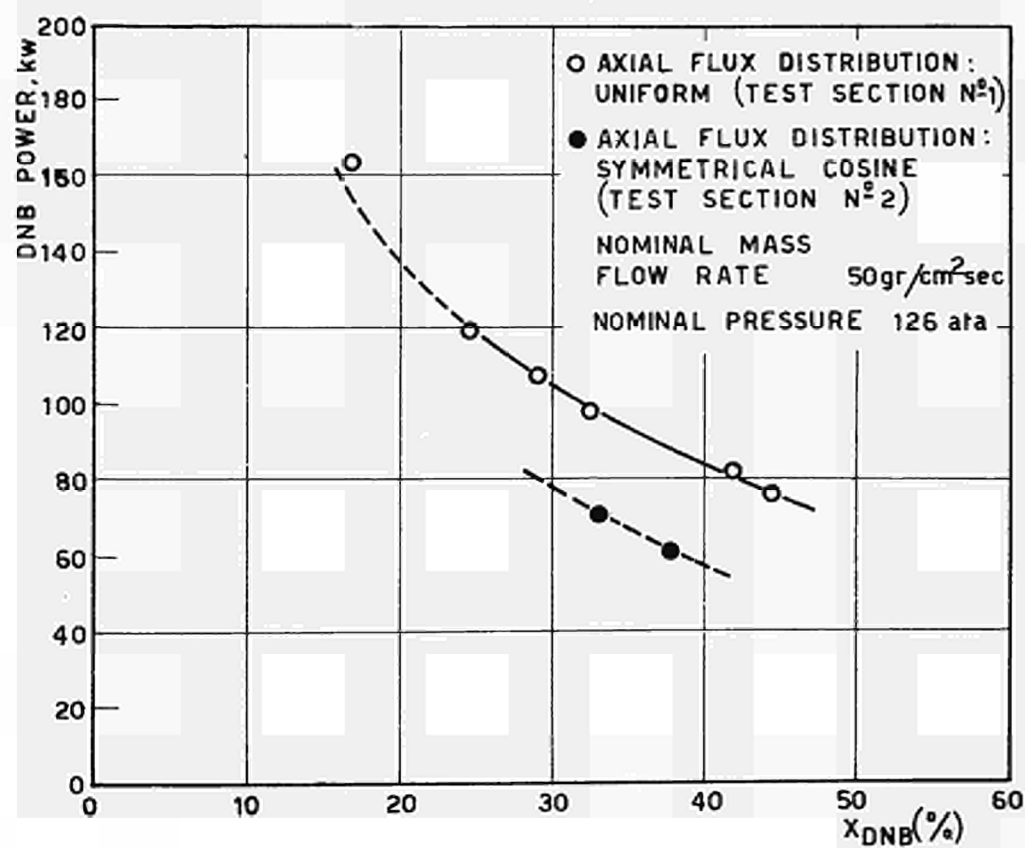
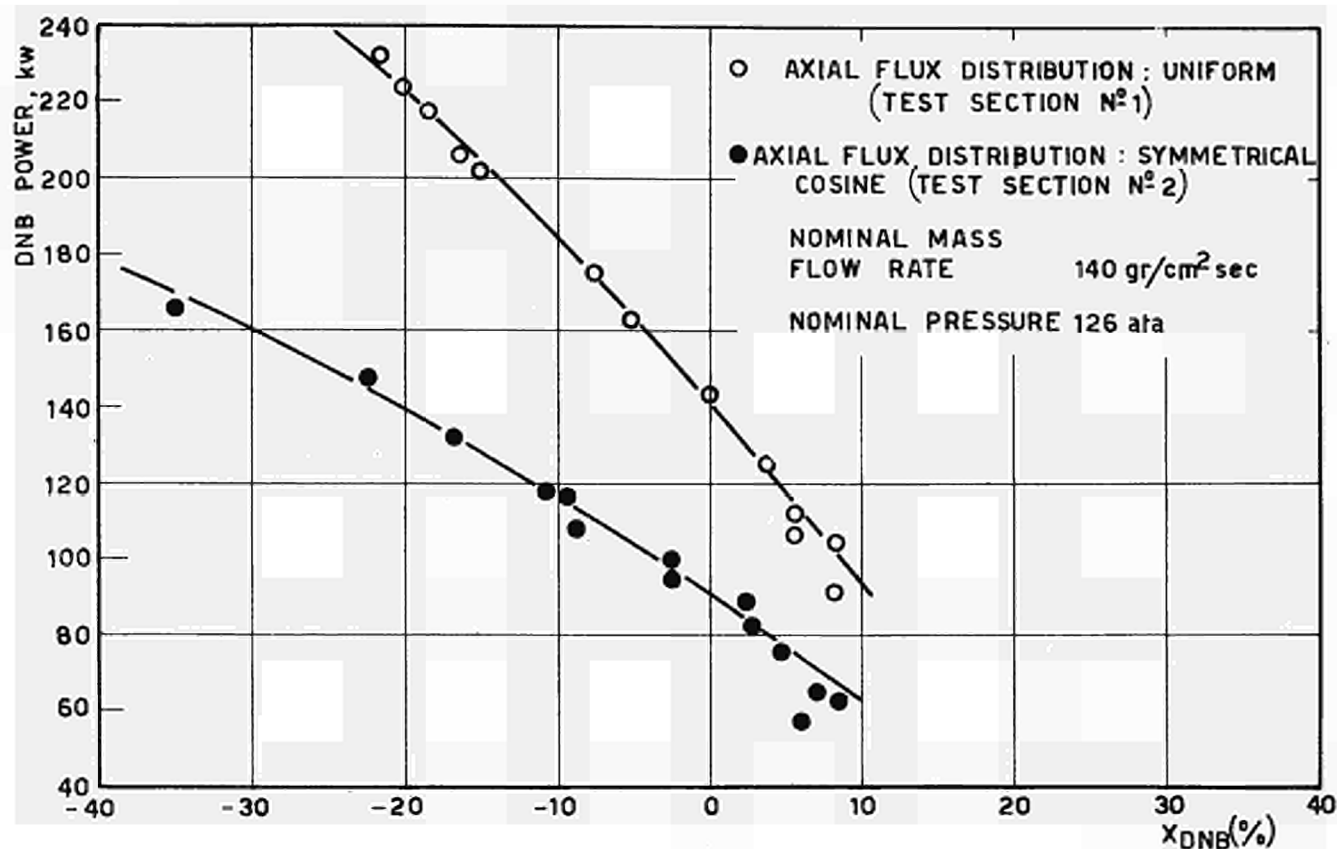


Fig 2.

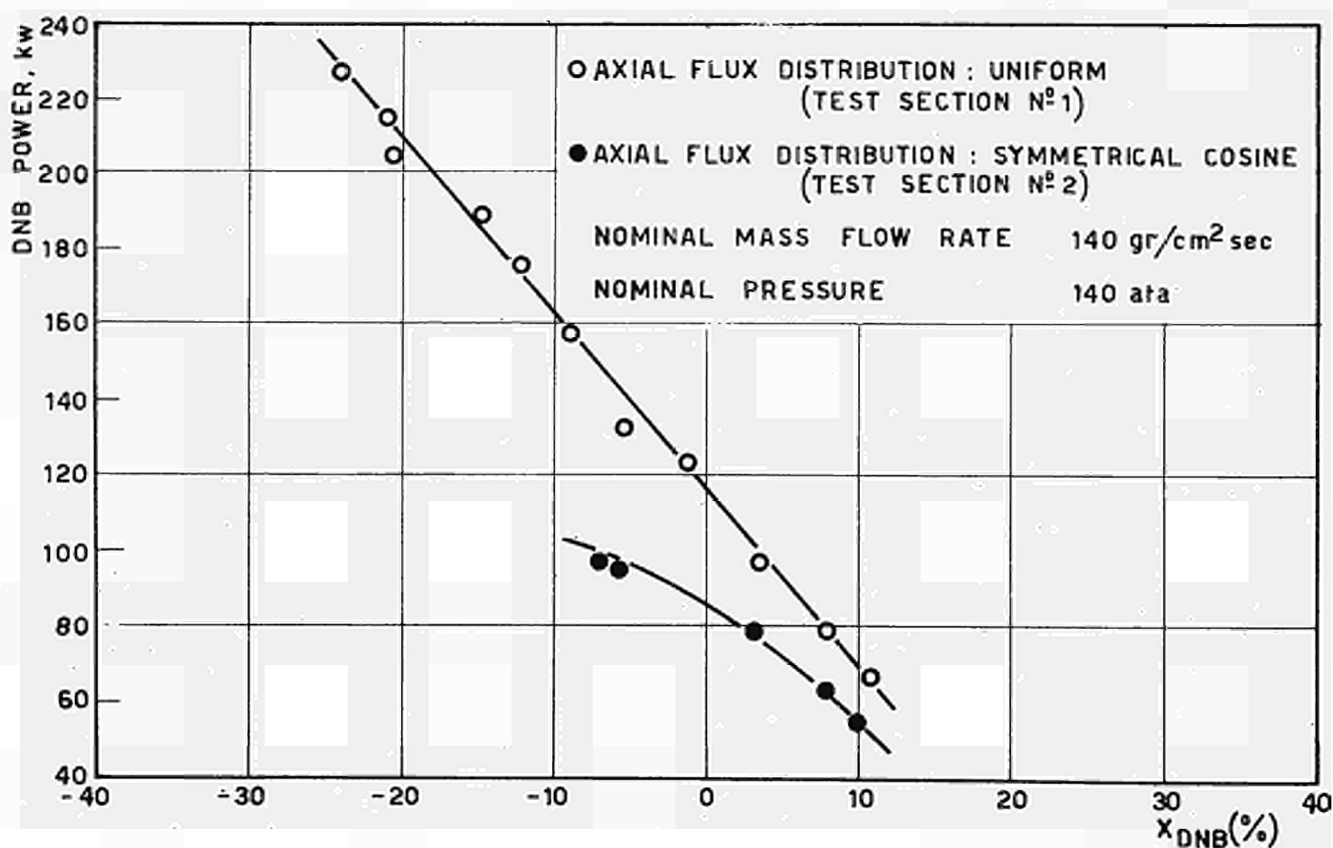
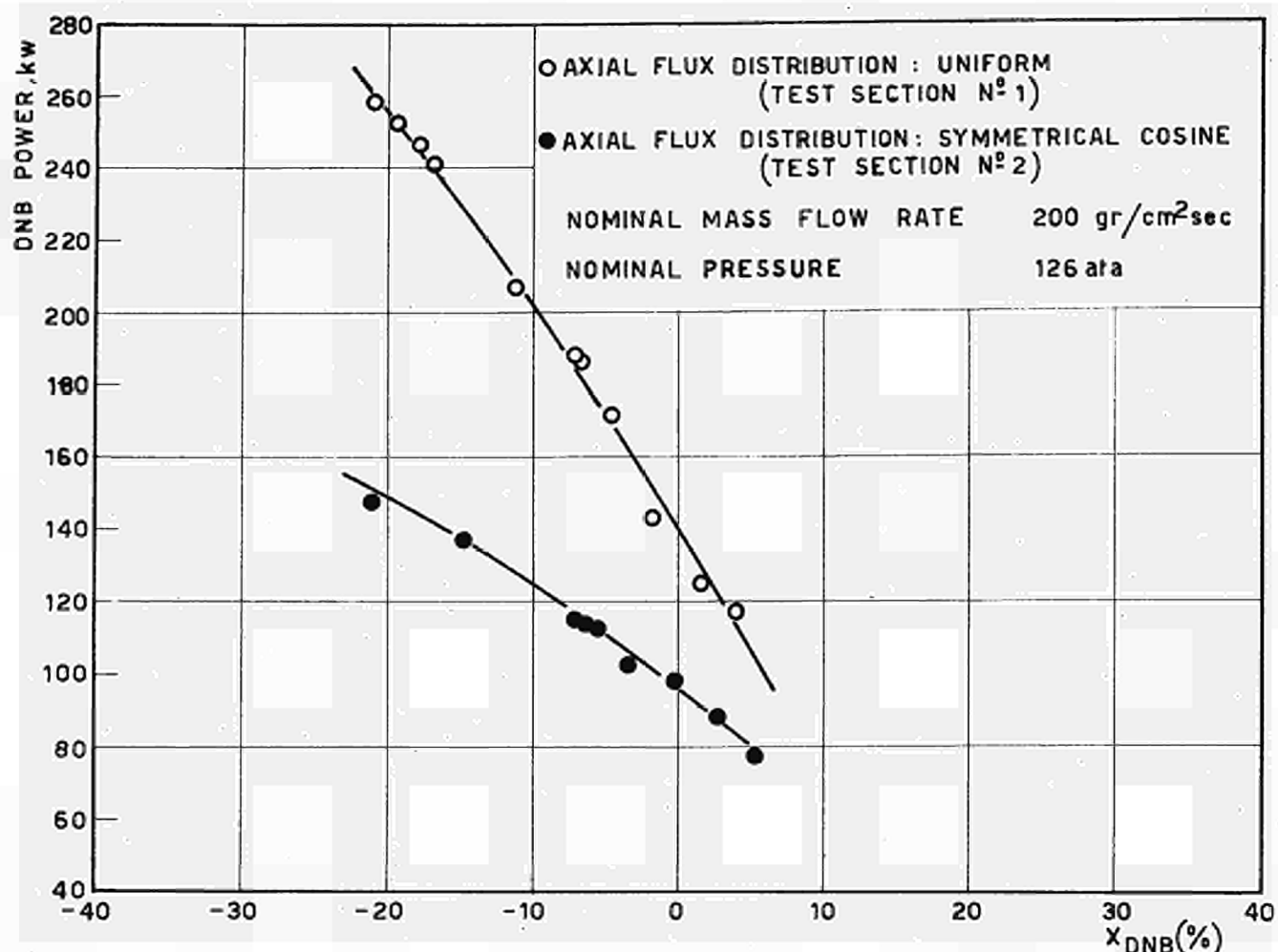


FIG. 3

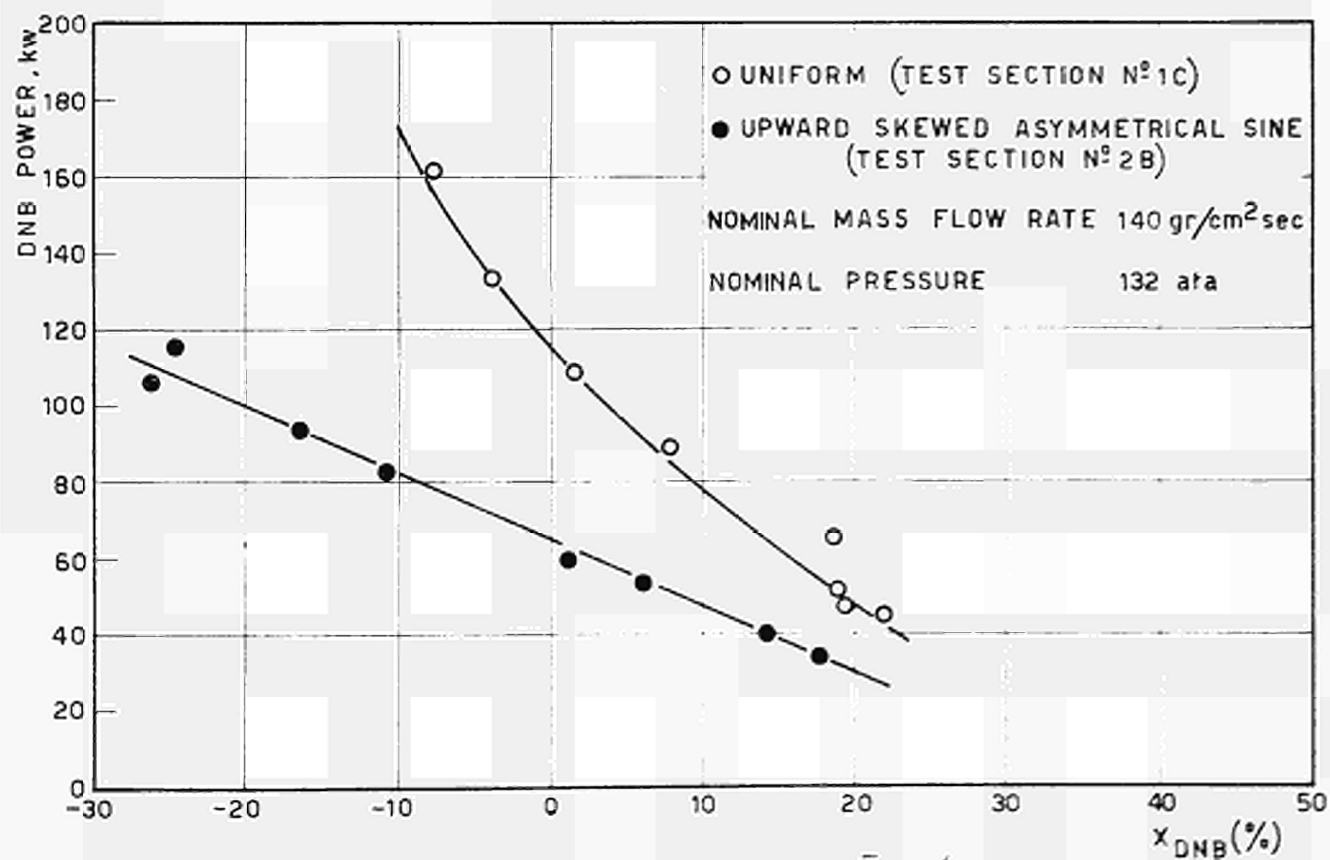
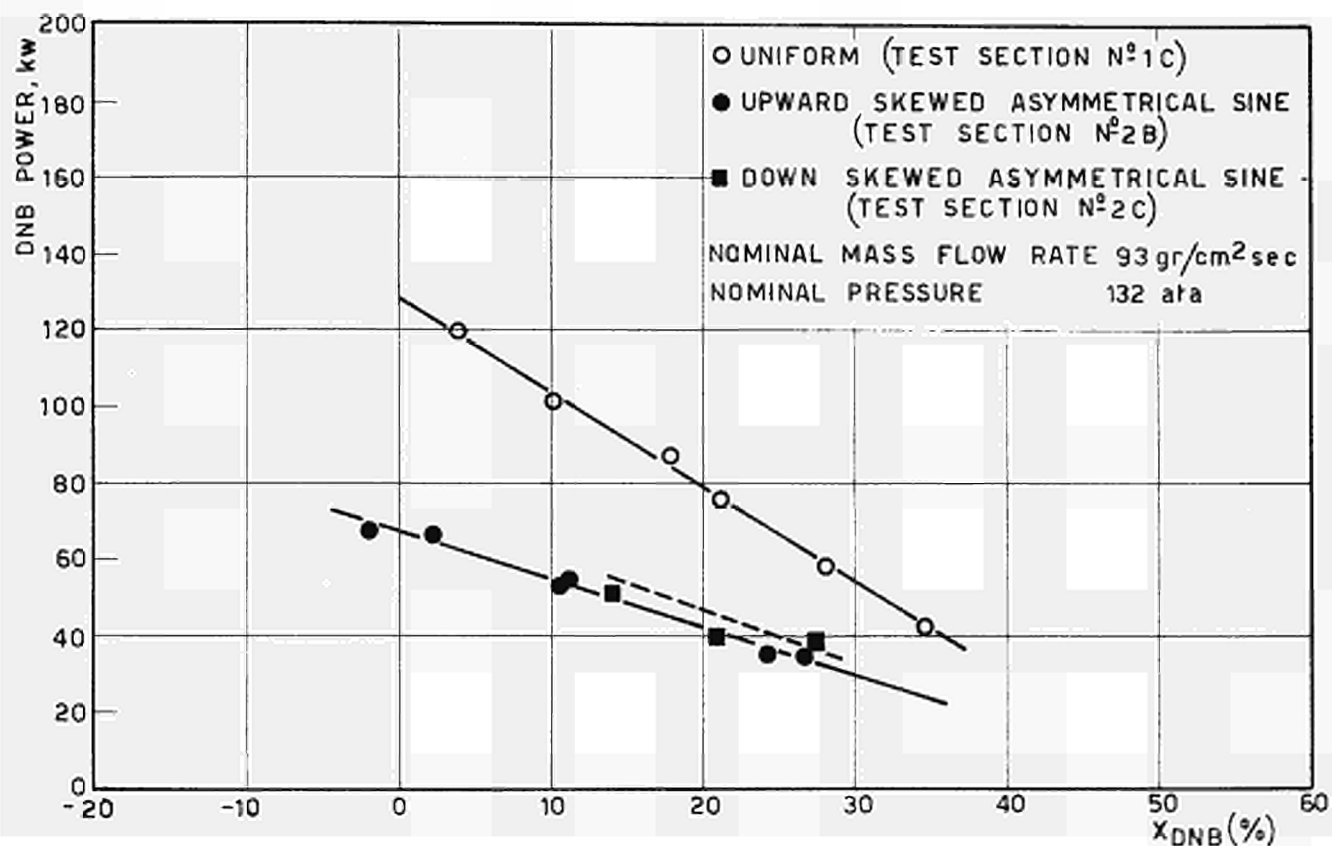


Fig. 4

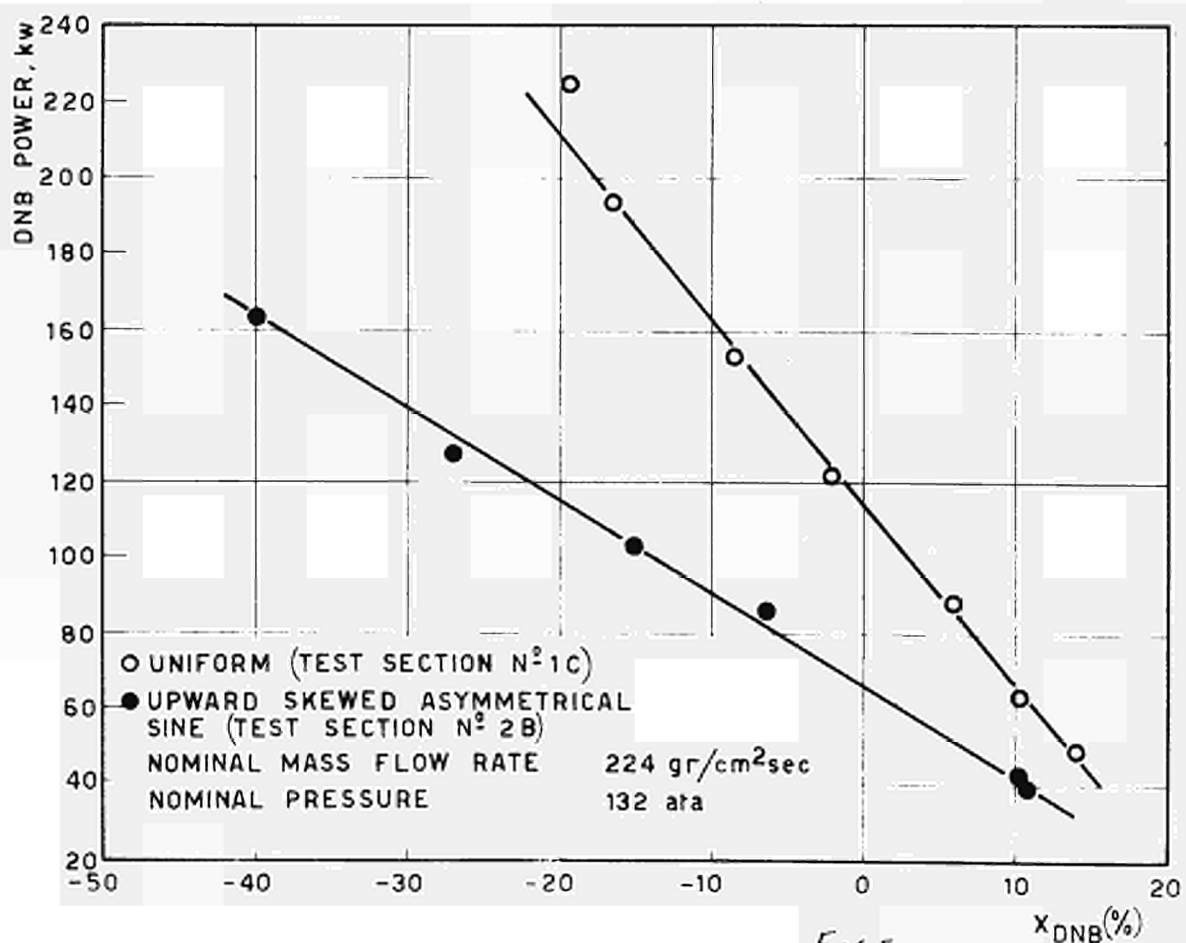
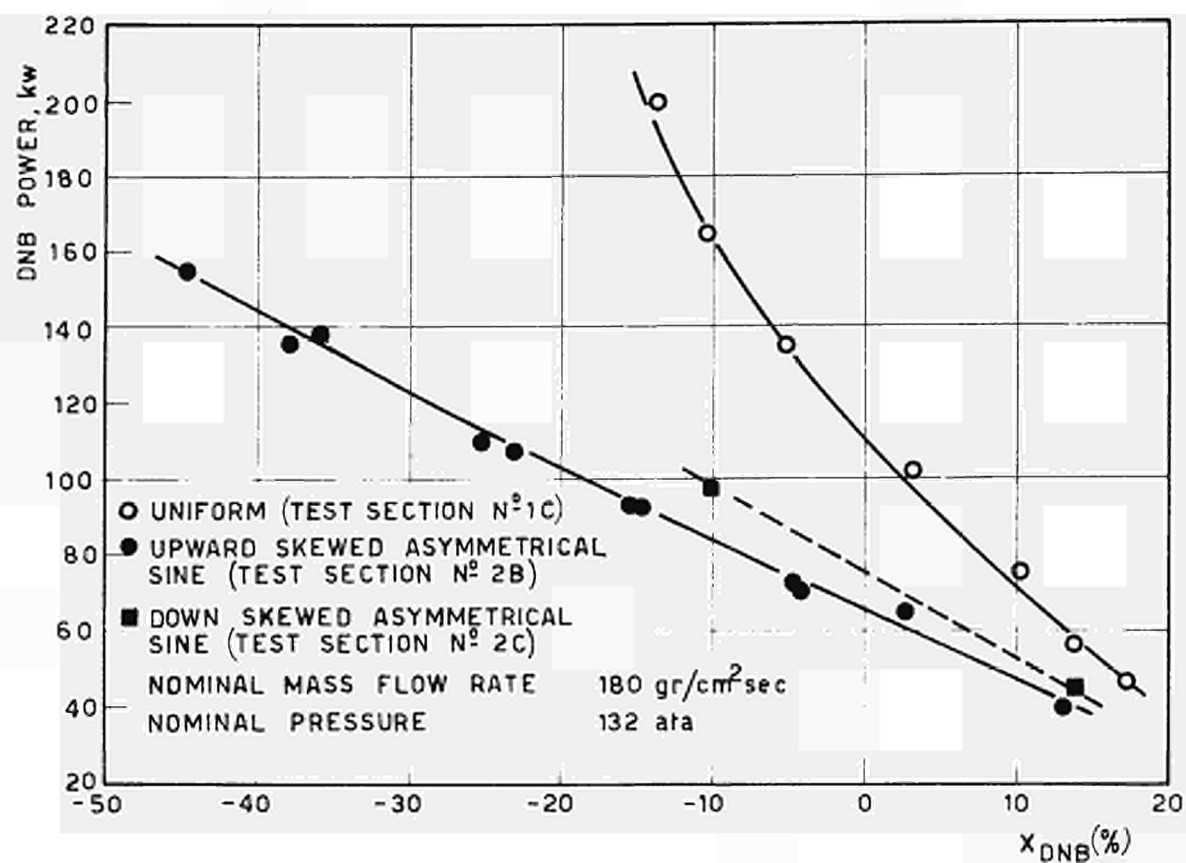


FIG. 5

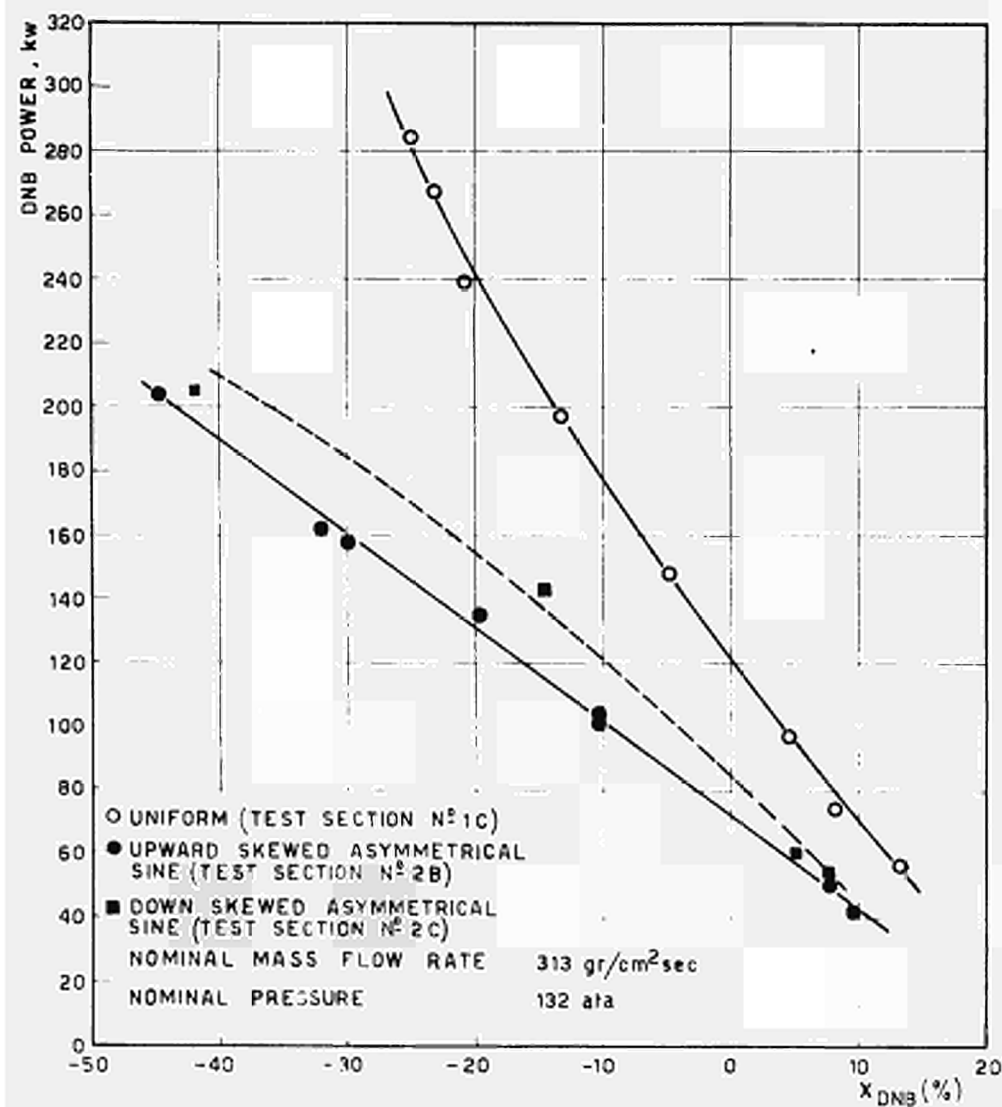


FIG. 6

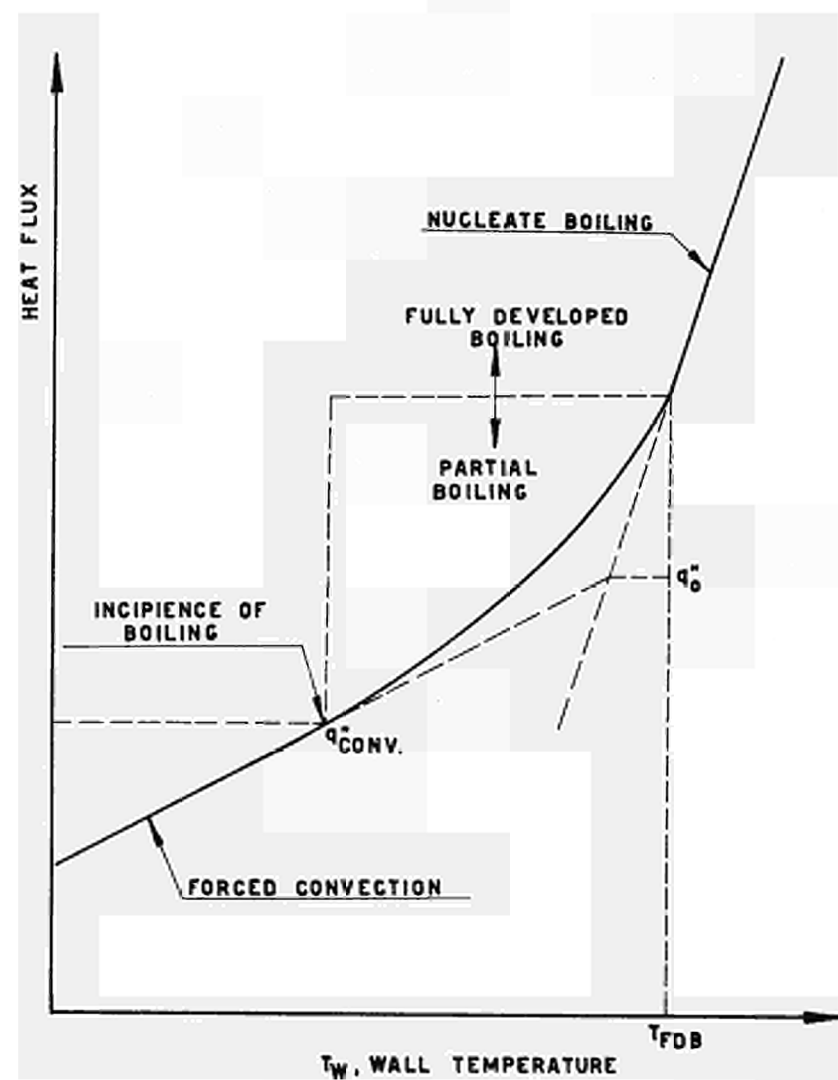
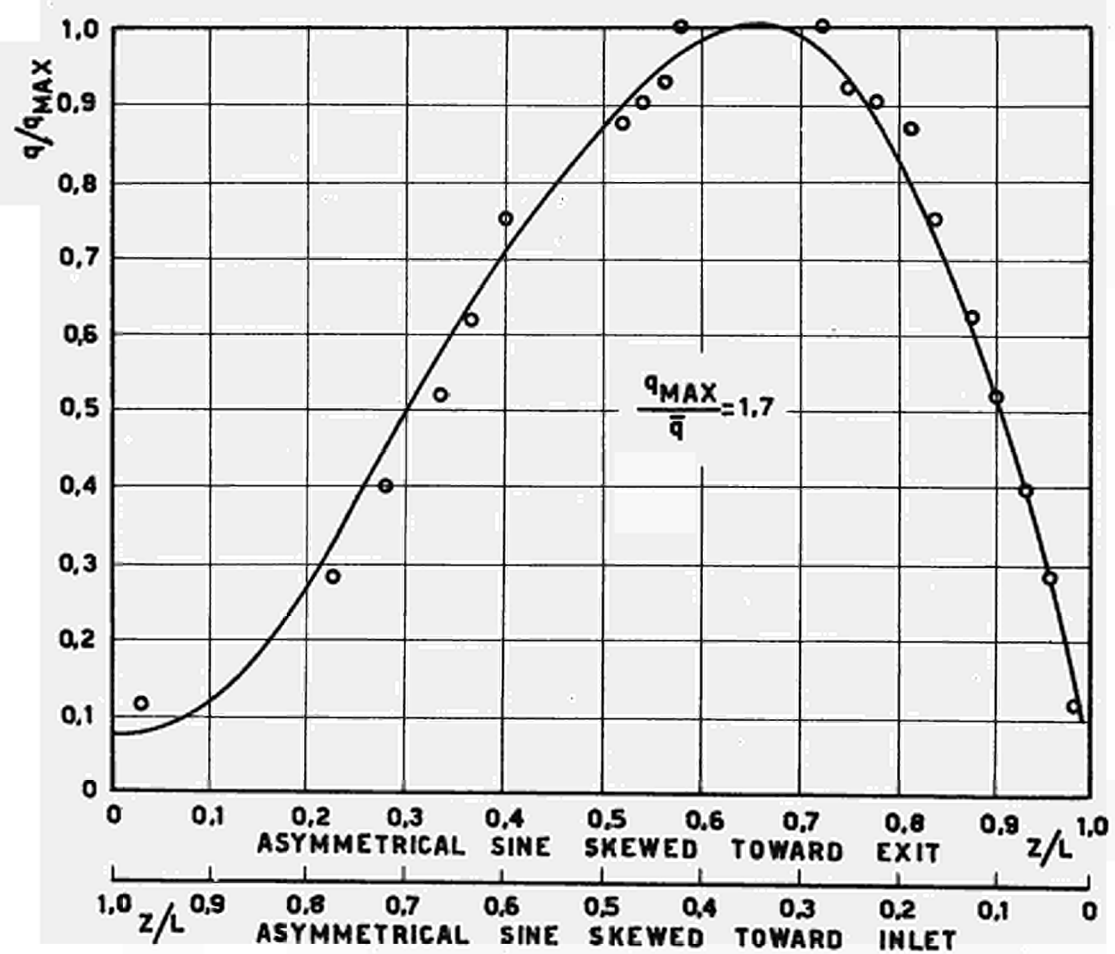
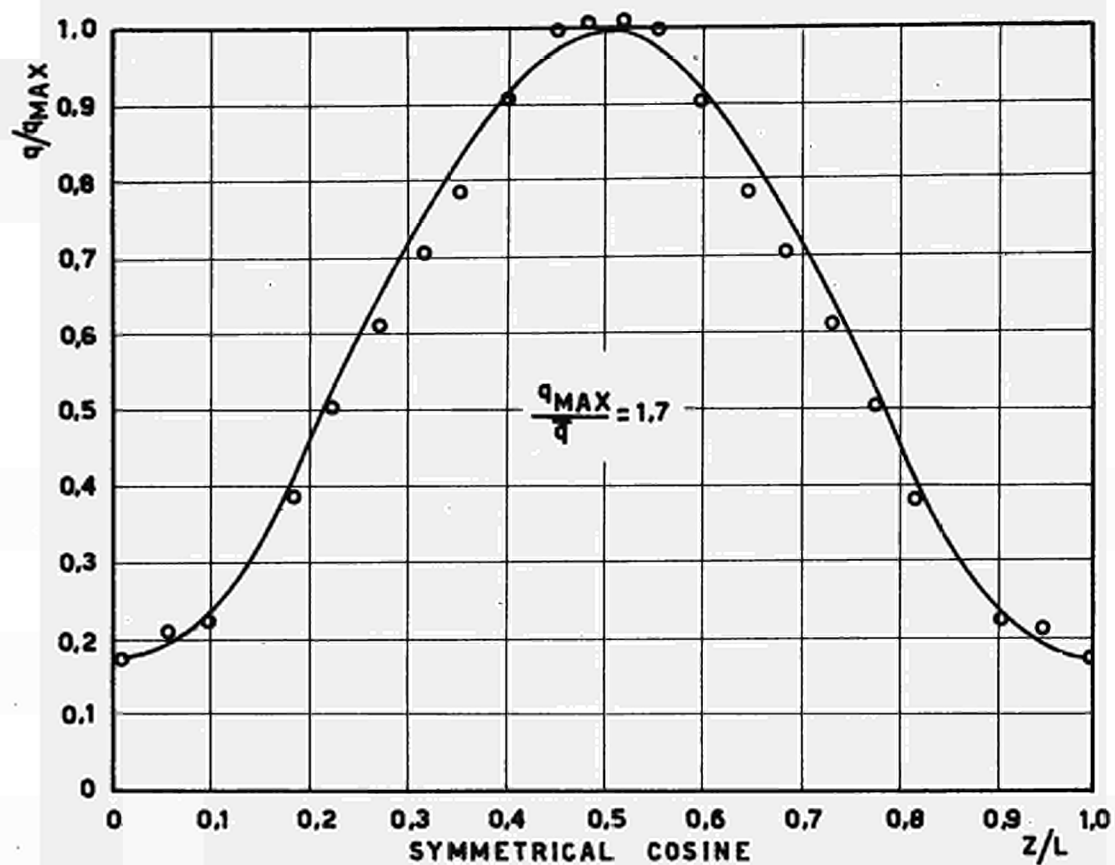


FIG. 7



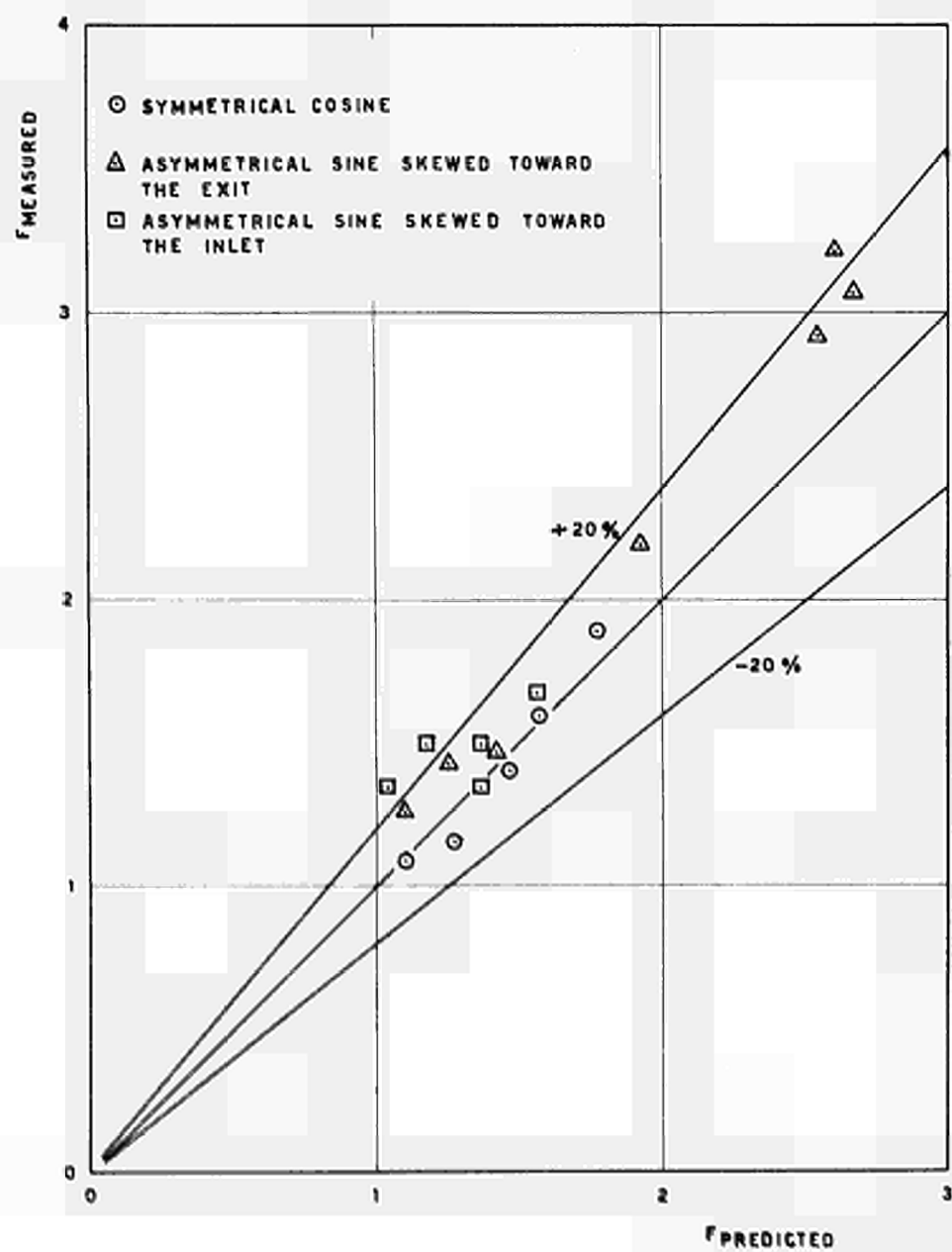


FIG. 9

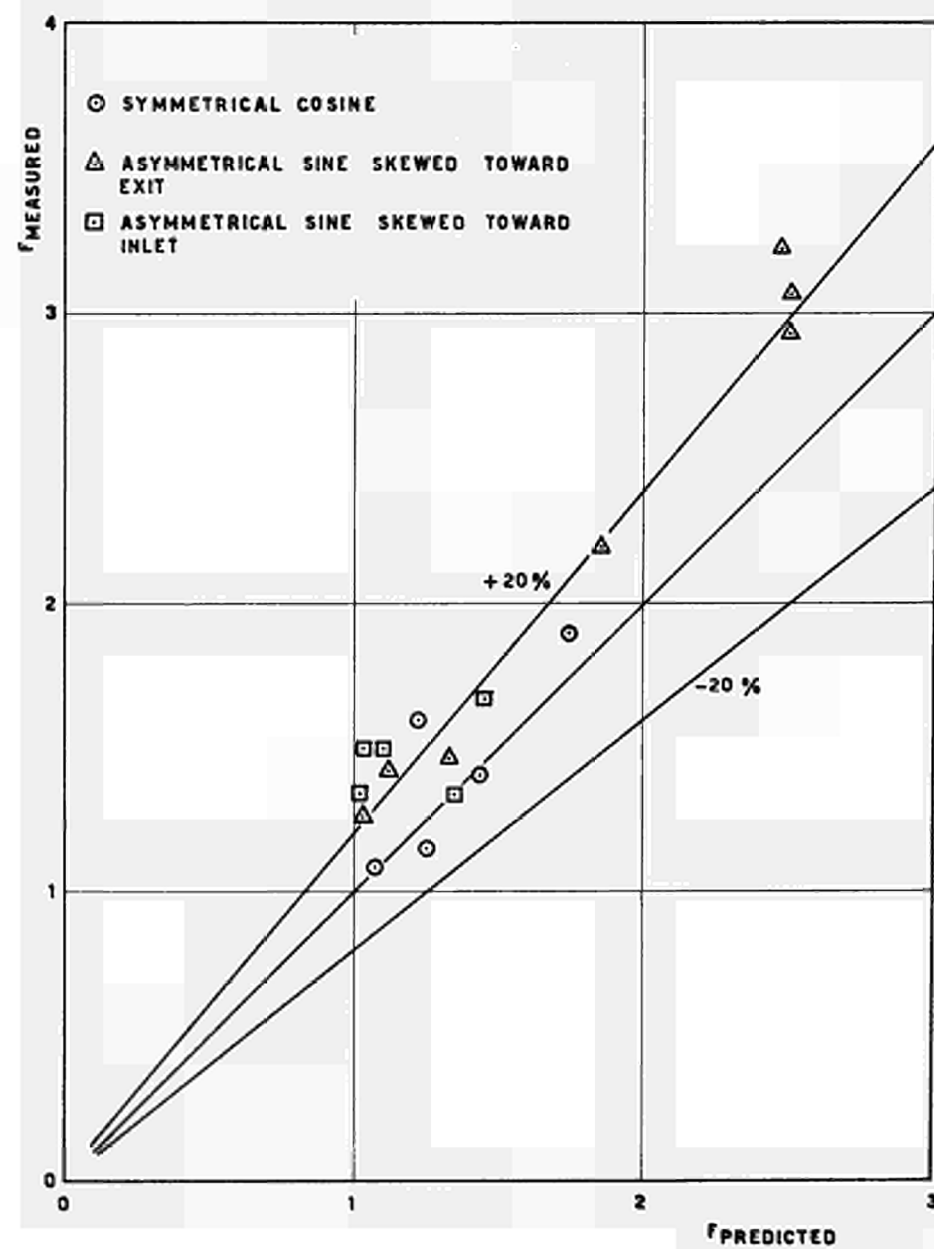


FIG. 10

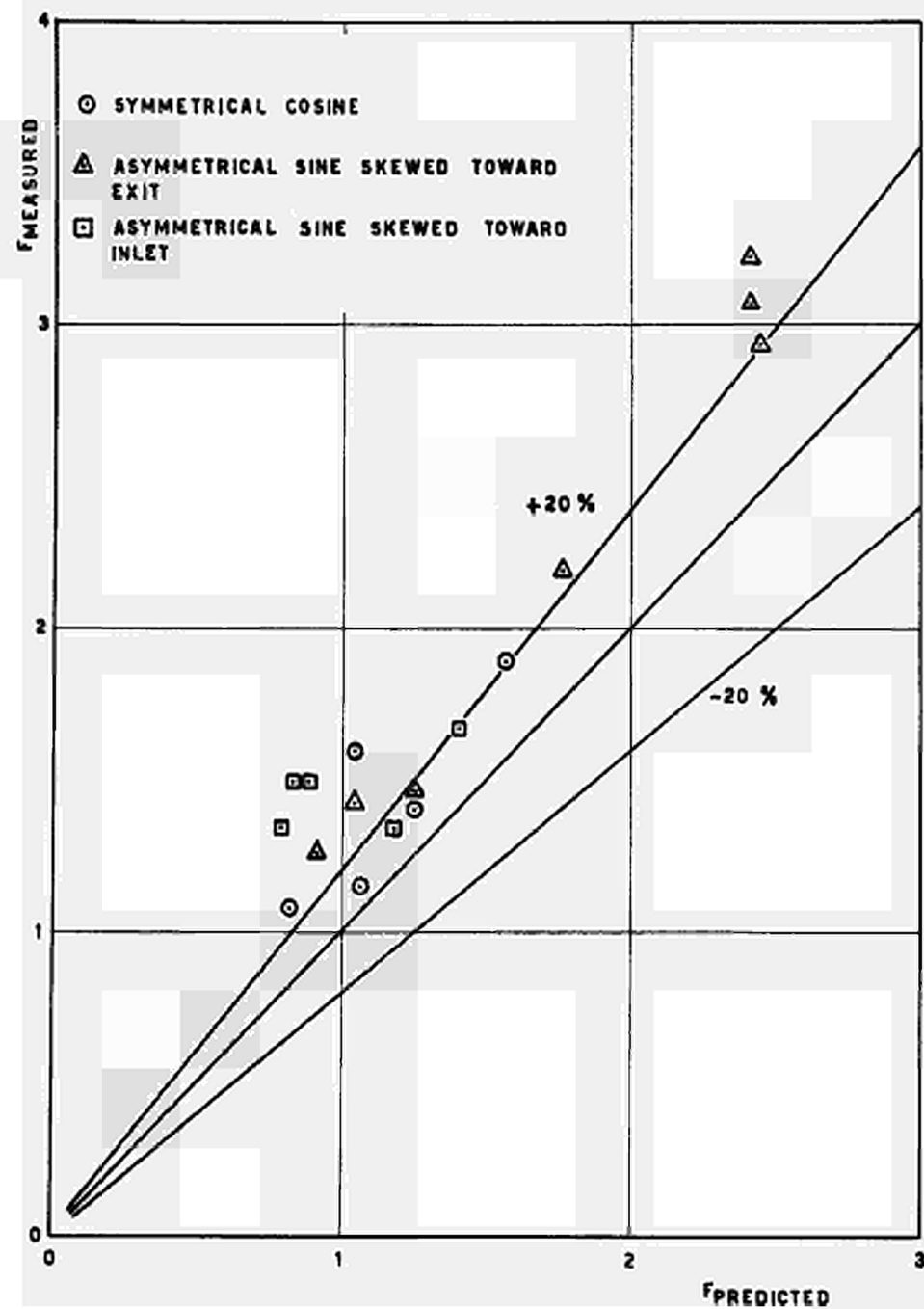


FIG.11

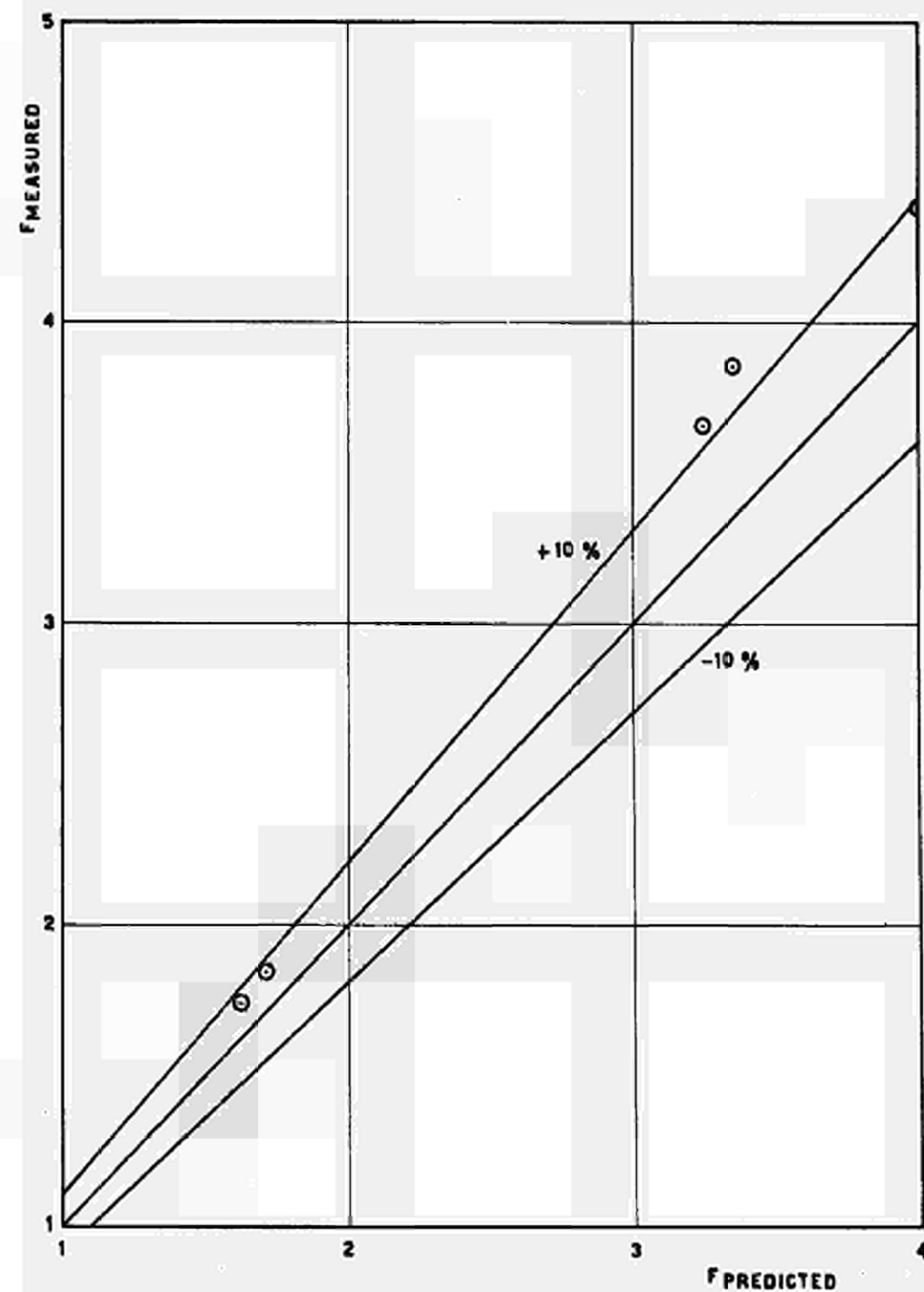


FIG.12

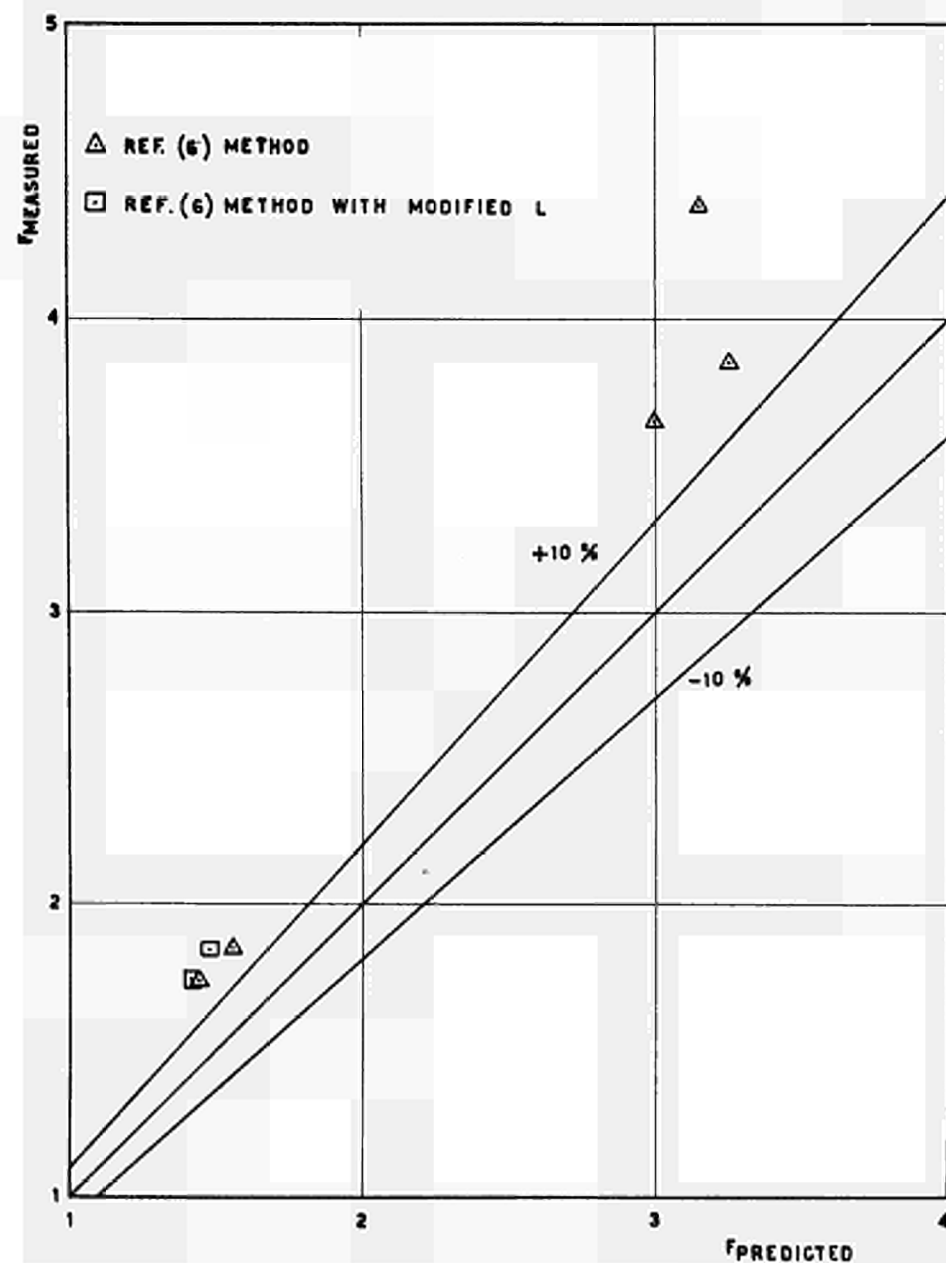


FIG.13

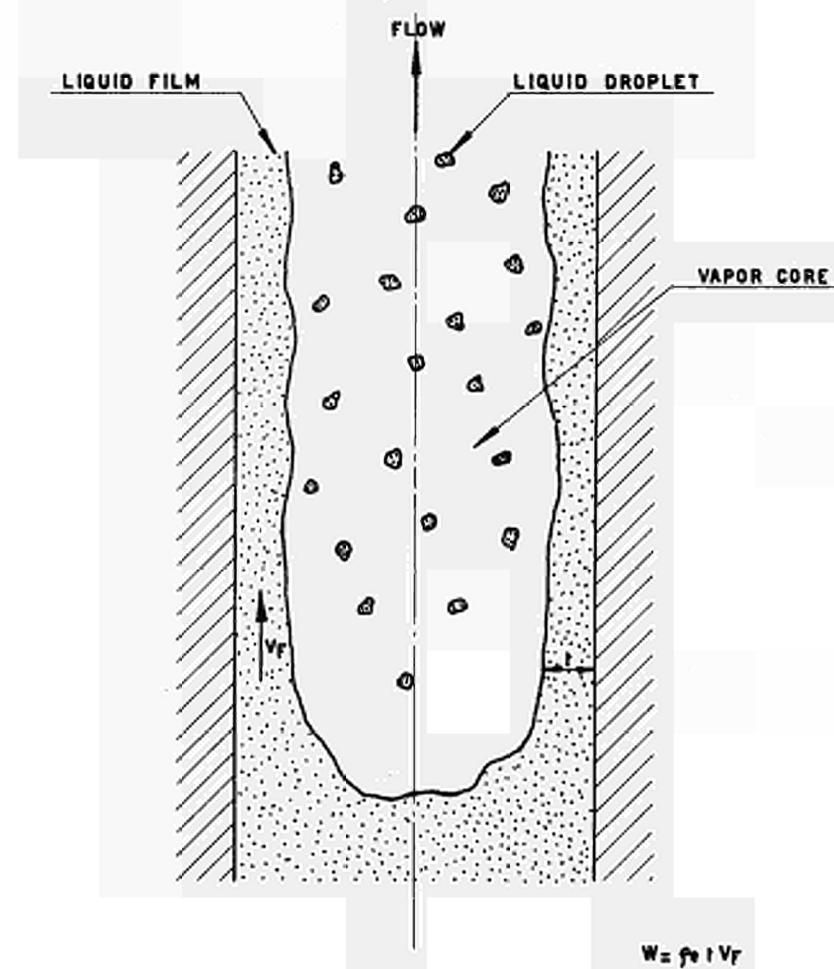


FIG.14

SERIES	q''_2 / q''_c	TOTAL HEATED L/D	
B	0, - 1,2	80	<p>Graph showing heat flux q'' versus normalized length L/D. The profile consists of a constant value q''_2 for the first 40 units, followed by a constant value q''_c for the next 40 units.</p>
C	0,16 - 0,5	78	<p>Graph showing heat flux q'' versus normalized length L/D. The profile consists of a constant value q''_c for the first 40 units, a constant value q''_2 for the next 28 units, and a constant value q''_c for the final 10 units.</p>
D	0,16	78	<p>Graph showing heat flux q'' versus normalized length L/D. The profile consists of a constant value q''_c for the first 40 units, a constant value q''_2 for the next 31,5 units, and a constant value q''_c for the final 6,5 units.</p>
E	0,16	78	<p>Graph showing heat flux q'' versus normalized length L/D. The profile consists of a constant value q''_c for the first 40 units, a constant value q''_2 for the next 18 units, and a constant value q''_c for the final 20 units.</p>
G	0,22 - 0,34	78	<p>Graph showing heat flux q'' versus normalized length L/D. The profile consists of a constant value q''_c for the first 68 units, followed by a constant value q''_2 for the final 10 units.</p>

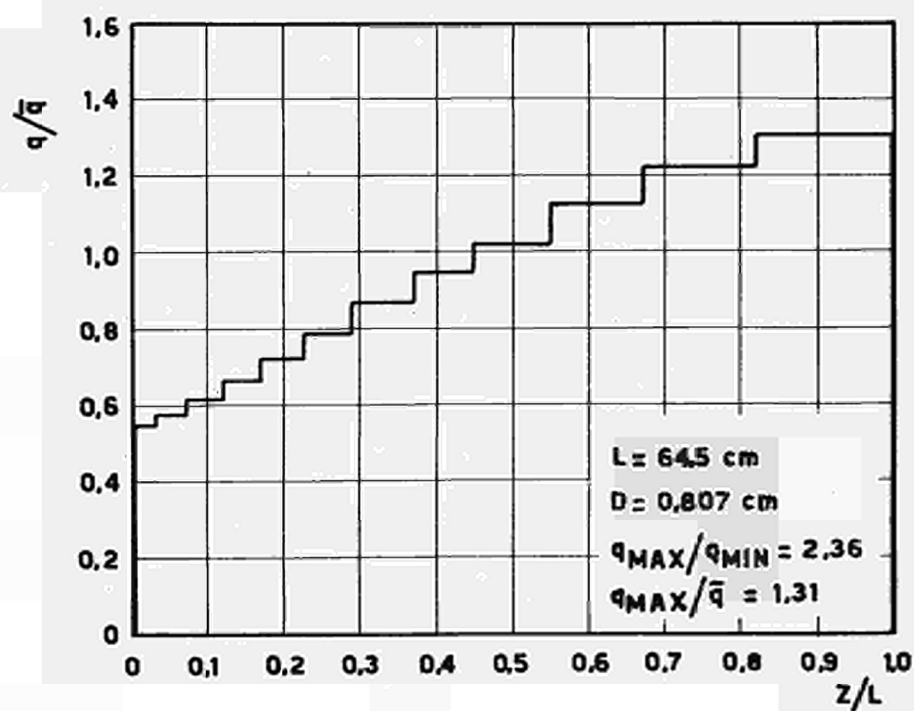
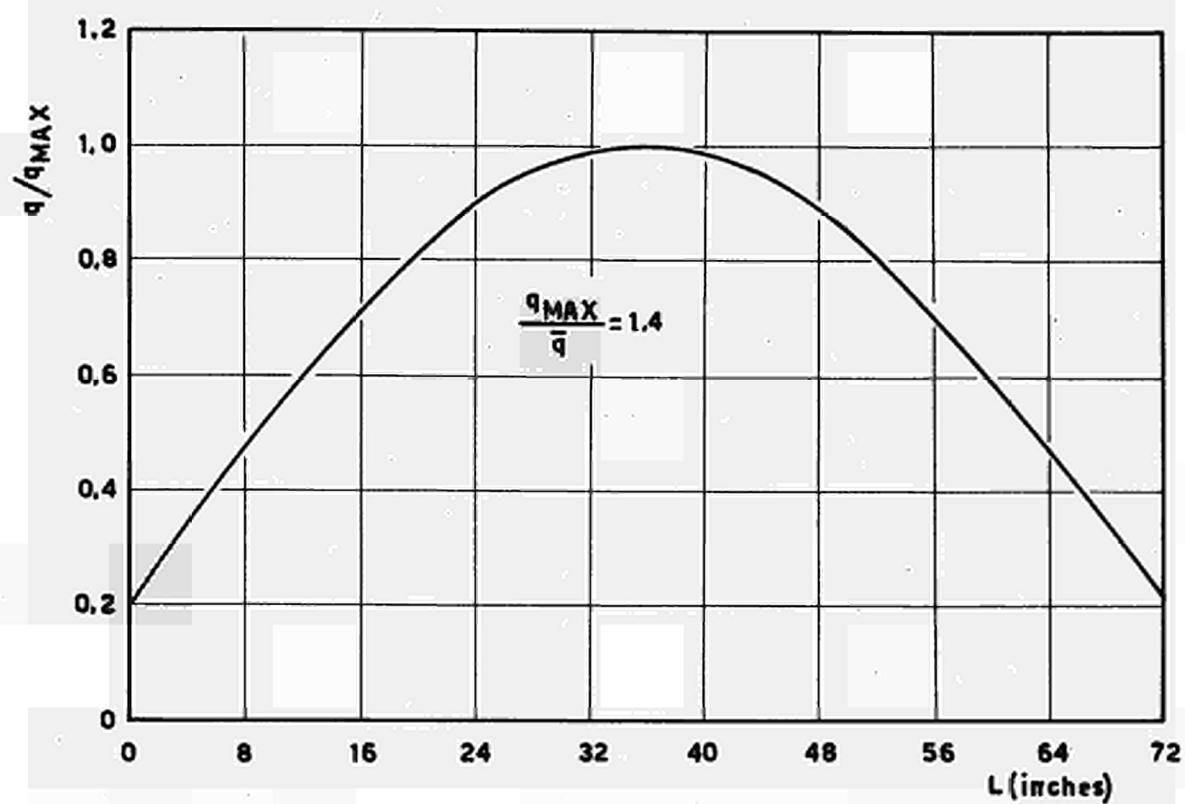


FIG. 16

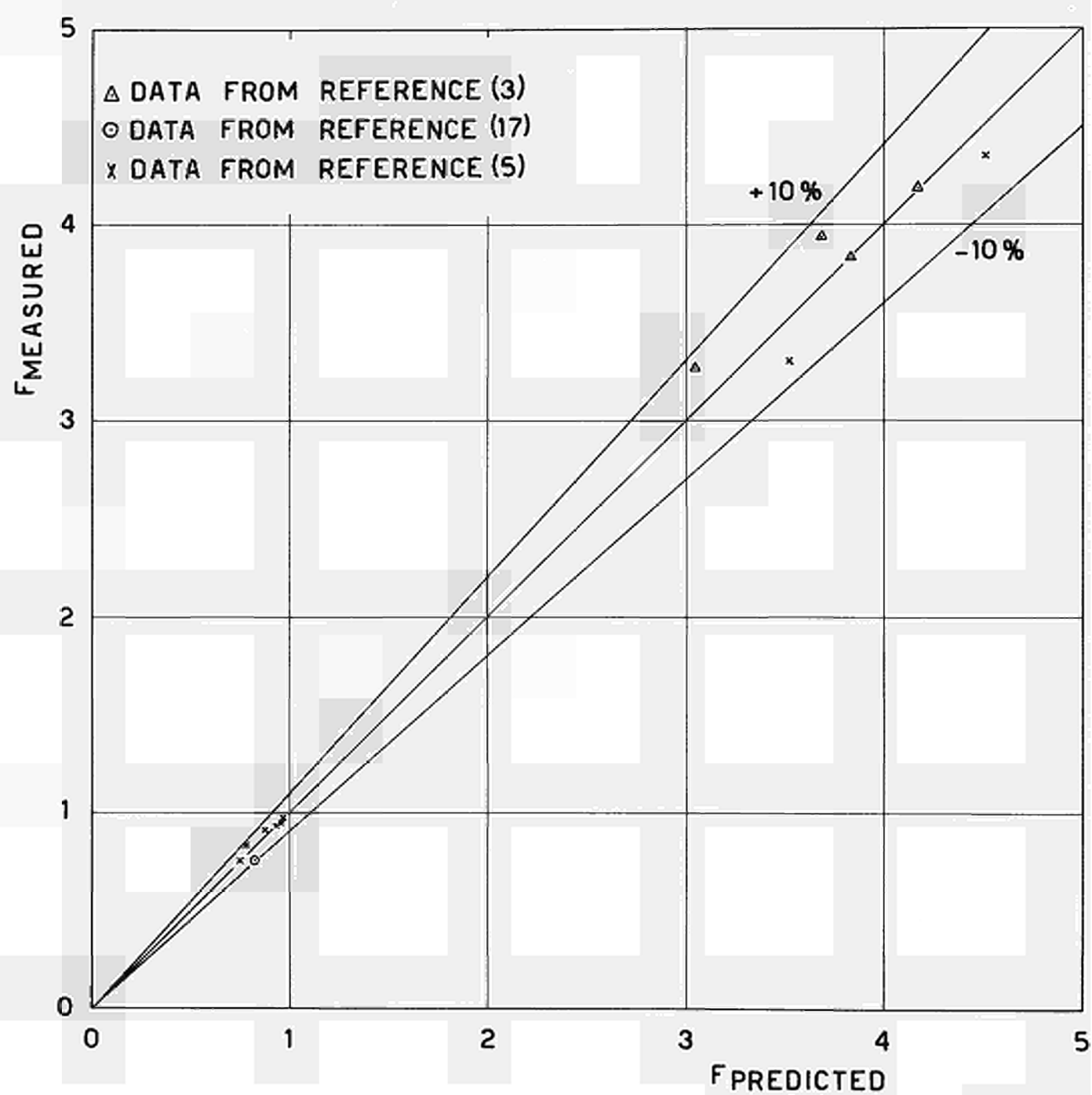


FIG. 17

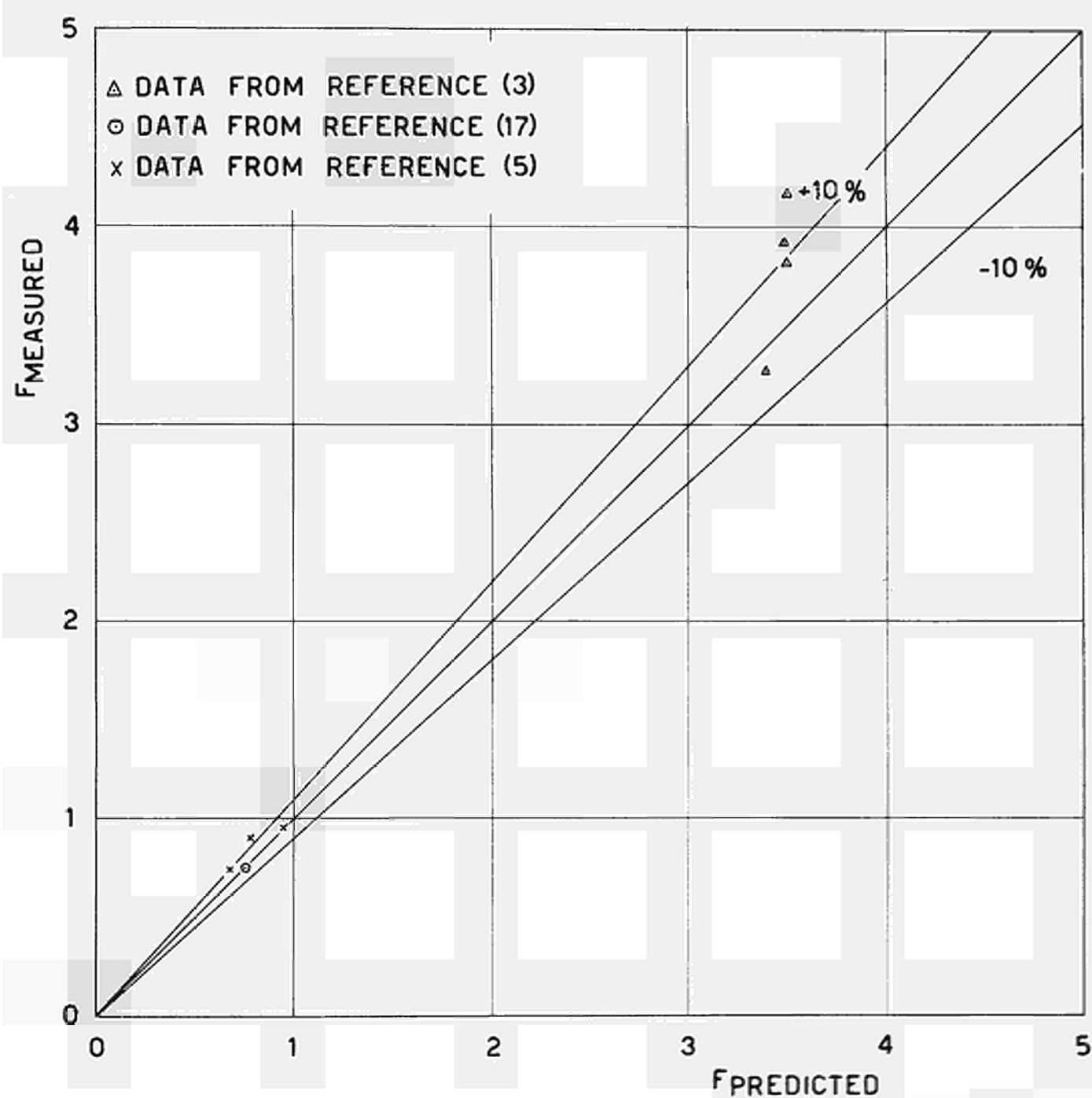


FIG.18

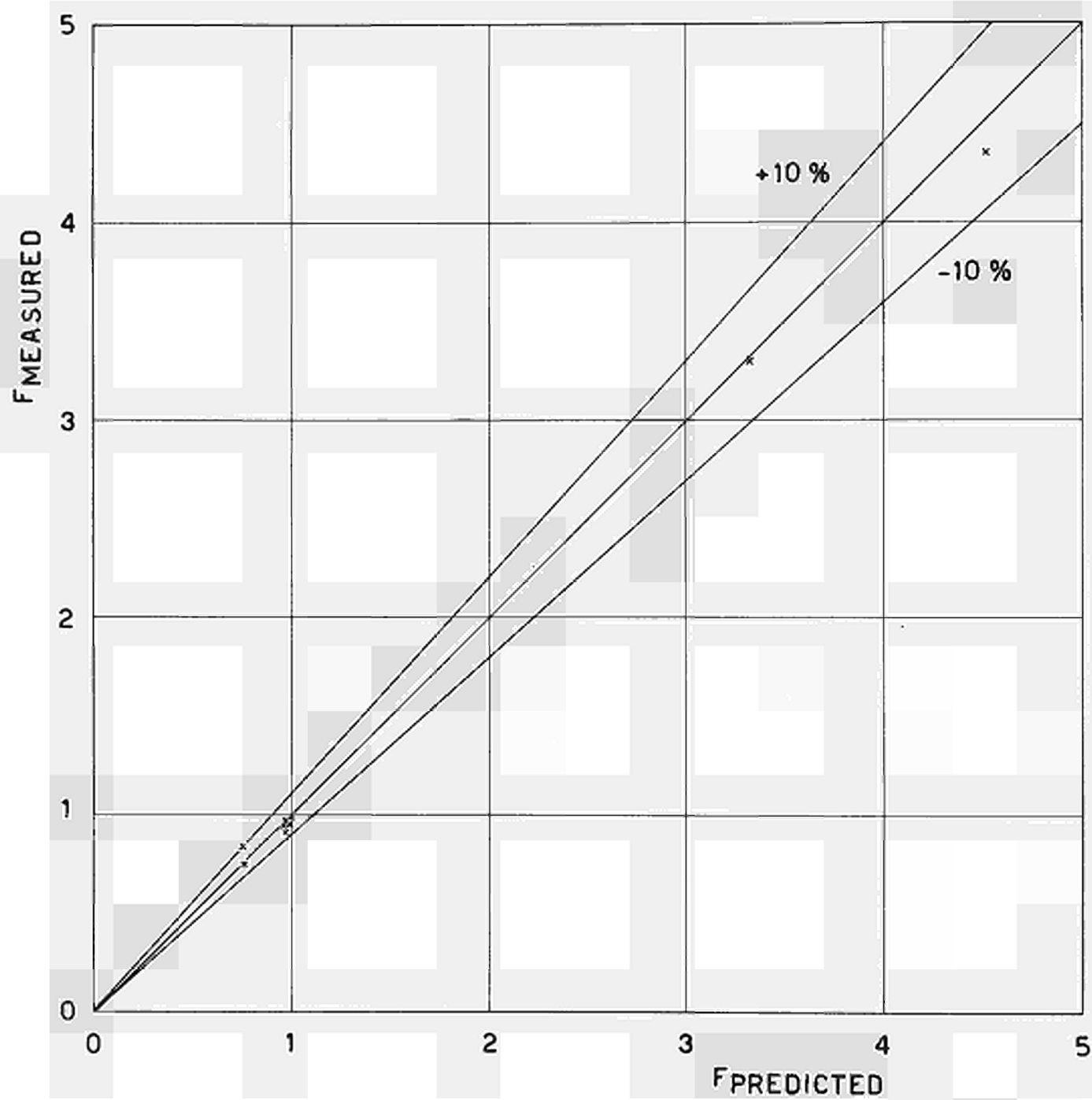


FIG. 19

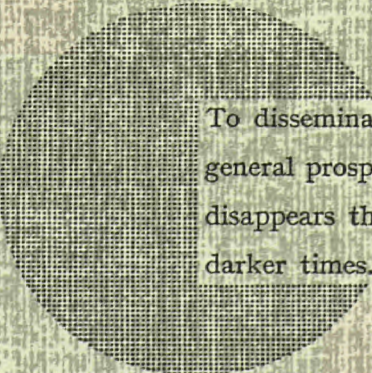
NOTICE TO THE READER

All Euratom reports are announced, as and when they are issued, in the monthly periodical **EURATOM INFORMATION**, edited by the Centre for Information and Documentation (CID). For subscription (1 year: US\$ 15, £ 5.7) or free specimen copies please write to:

Handelsblatt GmbH
"Euratom Information"
Postfach 1102
D-4 Düsseldorf (Germany)

or

Office de vente des publications
des Communautés européennes
2, Place de Metz
Luxembourg



To disseminate knowledge is to disseminate prosperity — I mean general prosperity and not individual riches — and with prosperity disappears the greater part of the evil which is our heritage from darker times.

Alfred Nobel

SALES OFFICES

All Euratom reports are on sale at the offices listed below, at the prices given on the back of the front cover (when ordering, specify clearly the EUR number and the title of the report, which are shown on the front cover).

PRESSES ACADEMIQUES EUROPEENNES

98, Chaussée de Charleroi, Bruxelles 6

Banque de la Société Générale - Bruxelles
compte N° 964.558,

Banque Belgo Congolaise - Bruxelles
compte N° 2444.141,

Compte chèque postal - Bruxelles - N° 167.37,

Belgian American Bank and Trust Company - New York
compte No. 22.186,

Lloyds Bank (Europe) Ltd. - 10 Moorgate, London E.C.2,

Postscheckkonto - Köln - Nr. 160.861.

OFFICE CENTRAL DE VENTE DES PUBLICATIONS DES COMMUNAUTES EUROPEENNES

2, place de Metz, Luxembourg (Compte chèque postal N° 191-90)

BELGIQUE — BELGIË

MONITEUR BELGE
40-42, rue de Louvain - Bruxelles
BELGISCH STAATSBLAD
Leuvenseweg 40-42 - Brussel

LUXEMBOURG

OFFICE CENTRAL DE VENTE
DES PUBLICATIONS DES
COMMUNAUTES EUROPEENNES
9, rue Goethe - Luxembourg

DEUTSCHLAND

BUNDESANZEIGER
Postfach - Köln 1

NEDERLAND

STAATSDRUKKERIJ
Christoffel Plantijnstraat - Den Haag

FRANCE

SERVICE DE VENTE EN FRANCE
DES PUBLICATIONS DES
COMMUNAUTES EUROPEENNES
26, rue Desaix - Paris 15^e

ITALIA

LIBRERIA DELLO STATO
Piazza G. Verdi, 10 - Roma

UNITED KINGDOM

H. M. STATIONERY OFFICE
P. O. Box 569 - London S.E.1

EURATOM — C.I.D.
51-53, rue Belliard
Bruxelles (Belgique)

CDNA03114ENC